ESCUELA TÉCNICA SUPERIOR DE INGENIERÍA (ICAI)

CONTRIBUTIONS TO THE IMPROVEMENT OF CAPACITY IN URBAN RAILWAY LINES

Autor: Ing. D. Luis Miguel Navarro Rodríguez

Directores: Prof. Dr. D. Antonio Fernández Cardador
Prof. Dra. Dña. María Asunción Cucala García

Madrid
June 2020

CONSTANCIA REGISTRAL DEL TRIBUNAL DEL ACTO

DE LA DEFENSA DE TESIS DOCTORAL

TÍTULO: Contributions to the improvement of capacity in urban railway lines

AUTOR: Luis Miguel Navarro Rodríguez

DIRECTORES: Antonio Fernández Cardador y María Asunción Cucala García.

TUTOR-PONENTE:

DEPARTAMENTO: Instituto de Investigación Tecnológica.

FACULTAD O ESCUELA: Escuela Técnica Superior de Ingeniería.

Miembros del Tribunal Calificador:

PRESIDENTE: Dr. D. **Firma**:

VOCAL: Dr. D. **Firma**:

VOCAL: Dr. D. **Firma**:

VOCAL: Dr. D. **Firma**:

SECRETARIO: Dr. D. **Firma**:

Fecha de lectura:

Calificación:

Extended Abstract

Nowadays, railway transport capacity is an important bottleneck for many railway operators that face its ever-increasing demand. This poses a challenge to existing lines as operation under conditions close to saturation tends to be unstable. Capacity in urban railway systems depends largely on dwell times at platforms, but capacity measures proposed in the literature rarely include the uncertainty associated to these times. On the other hand, the transport capacity of an urban railway line can be increased in many different ways. For planners and infrastructure managers it is vital to have at their disposal all the tools available that allow them to choose the most cost-effective solution among all the existing possibilities. This selection process can be complex sometimes and deciding how the available capacity should be increased is an important decision with significant financial consequences.

This work presents the uncertainty associated with Dwell Times modeled as fuzzy numbers; two new capacity measures are proposed: The Fuzzy Maximum Capacity and the Fuzzy Occupancy Time Rate. The proposed model makes use of a railway simulator that enables route compression to obtain the conflict-free compressed time of the section under study. Three practical capacity problems from the perspective of the railway traffic operator have been presented and solved. The new measures provide more information to the railway operator than the standard UIC method that does not include uncertainty regarding dwell times. Finally, the model has been applied to a section between Gràcia and Sarrià stations, belonging to the Spanish railway operator FGC.

This work also presents new transport capacity indicators suitable for urban lines that focus on disturbed circulation of trains; they can be used as a guide by decision-makers to help them decide on infrastructure capacity improvements. The indicators ease the process of deciding among different alternatives, considering the specific capacity improvement they involve individually. One of the advantages of this technique is allowing to decide among alternatives by choosing the most cost-effective solution to be implemented.

This project uses a simulation system capable of reproducing accurately the complete behavior of an urban railway installation like the FGC Barcelona-Vallès Line. The system models the behavior of the Rolling Stock operating in the railway line under the constraints defined in the design of the infrastructure and given a timetable and their operations definition. The model allows obtaining the minimum departure-arrival itinerary times in the stations under study. It has been applied to a case study in the

station of Provença that is a station with long Dwell Times during rush hour and belonging to the Spanish railway operator FGC. This case demonstrates the indicators application and their contribution; it also shows that it would be possible to extend the same kind of study to other nodes, allowing the systematization of their capacity improvement by fine-tuning their signaling system.

Contents

List of symbols

Symbol	Description
α_{obj}	Possibility Value
AHP	Analytic Hierarchy Process
APR	Absolute Position Reference
ATO	Automatic Train Operation
ATP	Automatic Train Protection
C	Capacity
$\tilde{C}$	Fuzzy Maximum Capacity
$C^{\underline{\alpha}}$	Lower limit α-cut of the fuzzy C̃
$C^{\overline{\alpha}}$	Upper limit α-cut of the fuzzy C̃
CBTC	Communications-Based Train Control
C_D	Disturbed Capacity
C_{ope}	Operative Capacity
CTC	Centralized Traffic Control
DT	Dwell Time
DTG	Distance to Go
ETCS	European Train Control System
ERTMS	European Railway Traffic Management System
FGC	Ferrocarrils de la Generalitat de Catalunya
HD	Average Disturbed Headway
I_{DA}	Departure-arrival itinerary time
I_{DAmin}	Minimum departure-arrival itinerary time
I_{DAP}	Average Disturbed Interval
N_{obj}	Necessity Value
OECD	Organization for Economic Co-operation and Development
s	Seconds
SWT	Scheduled waiting times
$\tilde{T}$	Fuzzy Dwell Time
T_{BT}	Difference of Departure Times between two consecutive Trains from two consecutive stations
T_{BTP}	Limit of perturbation of Difference of Departure Times between two consecutive Trains from two consecutive stations.
$Td^{\underline{\alpha}}$	Lower limit α-cut of the Dwell Time
$Td^{\overline{\alpha}}$	Upper limit α-cut of the Dwell Time
T_{D1A}	Time of departure of 1st train from station A
T_{D2B}	Time of departure of 2nd train from station B
T_{Dk}	Dwell time at each platform k

$\tilde{T}_{Dk}$	Fuzzy Dwell time at each platform k
$T_{Dk}^{\underline{\alpha}}$	Lower limit α-cut of the dwell time at each platform k
$T_{Dk}^{\overline{\alpha}}$	Upper limit α-cut of the dwell time at each platform k
T_{DL}	Support of the Fuzzy Dwell Time distribution
T_{ope}	Operation time cycle
T_R	Train Running Times
T_{RD}	Disturbed Train Running Times
$\widetilde{U}$	Fuzzy Occupancy Time Rate
U_{UIC}	Maximum Occupancy Time Rate recommended by UIC
UIC	International Union of Railways

Acknowledgements

"*Per Aspera ad Astra*"

After these years of doctorate studies, I analyze my personal development and realize this has been actually a very special stage of my life. Since the beginning this has been a great personal challenge. During undergraduate education I managed to see a relatively clear and structured path through them. But research is quite a different thing as the aforementioned path is sometimes blurry and almost always unfamiliar. Also, it has not been especially easy for me to balance a full-time work, my other life commitments and this research development all at the same time. Actually, many cups of tea have witnessed this fact during uncountable night-time working hours devoted to developing this research.

First and foremost, I would like to express from the bottom of my heart my sincere gratitude to my thesis directors Antonio and Paloma for their dedicated guidance and continuous support through each stage of this process. There were some moments when the research path was not completely clear for me. I already had a general vision about what I wanted to investigate but it was not so clearly defined yet. The image in my mind was still shadowy. So, the advice and supervision of my directors helped me greatly to clarify the path of this dissertation research. And their skillful guiding hand helped me to never lose hope along the way.

I would also like to thank the Comillas Pontifical University and all the staff members for their support during all this process, especially their assistance with all the administrative procedures required. Also, for all the resources placed at my disposal to developing this work.

I would also like to express my gratitude to FGC (Ferrocarrils de la Generalitat de Catalunya) and especially to Mr. Pedro Barea for the advice received regarding the operation of their lines and their support with the definition and design of the simulator. This has been a key asset of this work; a real-world simulated environment can be only as faithful as the precision of the real data we use to generate it.

Also, I am profoundly grateful to several teachers I had during my primary and secondary education. Now looking back, I clearly see that they managed to lay the foundations of this research by sowing very early into me the seeds of scientific curiosity.

Last but not least, I would like to thank my family and friends for their support not only

during this research but also in many different moments of my life in general. These are not things we should ever give for granted and truly deserve our daily appreciation.

And I also need to mention those who are not among us anymore but will eternally be present in our hearts. Quoting Antoine de Saint-Exupéry: “He who has gone, so we but cherish his memory, abides with us, more potent, nay, more present than the living man”.

A mis luceros arriba en el cielo, siempre conmigo.

CHAPTER 1

INTRODUCTION

The process of interconnection of different parts of the world, movement and integration of goods and people among different countries is what we name nowadays as Globalization. The beginning of the twenty-first century has seen a progressive acceleration of this process, which impacts global emissions of greenhouse gases by increasing them. There is a growing concern regarding these increments and future policies may be oriented to limit greenhouse gases emissions and therefore boost means of transport that can be more environmentally friendly like rail transport. Rail has the key advantage of emitting less than most of other transportation methods. And these emissions can be further reduced with the transition to a 100% renewable electricity system of production. So, it is imperative to find new solutions that allow increasing the use of rail, which is potentially the most environmental conscious form of transport. And with this increase, accelerate the shift of passengers and freight from air, sea and road to rail.

Furthermore, future projections devise a global trend of general increase in populations living in major cities. These projections are going to challenge existing railway installations that will experience great difficulties to cope with the aforementioned demand increase. Hence, the increase in railway congestion due to this demand surge needs to be planned out very carefully by railway operators.

The European Union has adopted four railway packages with the aim of gradually opening up rail services to a higher degree of competition by defining a common framework of standards that allow a development of a single European railway zone. In the end and among other features, this initiative will reduce barriers by increasing interoperability between countries. This in turn will lead to an additional increase in railway capacity demand. Also, from the European Commission there is a decided drive to support rail to increase its importance in reducing the environmental footprint of the whole transport sector, as it is a very efficient sector and largely electrified.

Railway transport is nowadays in the process of improving elements like its efficiency, level of customer satisfaction, quality of service and capacity. Regarding the latter, many installations are reaching their maximum allowed capacity levels and future projections show that this trend will continue into the following years. Thus, it is of prime importance that railway infrastructure managers face as soon as possible the challenge of reevaluating their available capacity and take decisions in order to increase the available capacity in the railway installations that they manage.

But this capacity expansion tends to be a process that is very intensive in capital, therefore planning the investments well in advance is normally mandatory as its implementation needs planning and execution times that tend to be long. Also, financing is sometimes complicated and subject to political winds that can be many times quite variable.

Therefore, before starting costly capacity increase programs through the purchase of new Rolling Stock, refurbishing or update of Signaling Systems or even completely new lines, other much more cost-effective solutions must be considered. This actually means squeezing more juice out of the current installations, before they have to be remodeled partially or completely. To do so, and therefore before deciding among different projects to expand line capacity, infrastructure managers need to use capacity indicators that allow them to choose efficiently the available options that they have at their disposal.

Some railway administrations - like the Spanish FGC – are in the process of updating their infrastructure to cope up with the growth in passenger demand. The current scenario, in which governments are pushing the trend to limit the use of private cars in order to reduce pollution levels in urban areas, for example by means of creating zero-emission zones, is gradually increasing pressure on passenger demand in the railway infrastructure.

For example, in 2019 FGC underwent an increase in passenger demand of 4,4% in comparison to the previous year, which in turn also experienced an increase of 3,5% in comparison to the previous period. As a response to this increasing pressure, FGC announced on June 2019 that they were planning to invest 300 million euros to renew their lines with the aim of increasing available capacities of their lines. The rhythm of investment is expected to be of 100 million euros per year until 2021. A big part of this money will be spent on new trains and some station renewals, like the redesign of Plaça Catalunya, which is one of the busiest stations of the line. But many times, capacity bottlenecks in railway lines are not present where they seem to be at first sight and a more profound analysis is required to pinpoint their exact position. Therefore, infrastructure improvements require the use of tools that ease the process of decision among different investment possibilities. In this scenario is where capacity indicators show their valuable contribution.

Specifically, when it comes to urban railway lines, these lines have some common features that make it difficult to apply standard capacity indicators. These indicators do not reflect some of the intrinsic aspects present in urban lines. These are:

- Dwell Times at stations have a huge impact in capacity, due to their variability and the high values they can reach in crowded stations specially during the rush hour of the service. The impact of this effect is dramatically increased as urban lines tend to have very short sections between stations; in urban sections the average distance between stations is typically about 800m. This implies that Dwell Times have a remarkable effect on minimum running times of trains.

- In urban lines that are close to saturation during the rush hour, it is frequent that train movements are disrupted by the previous train in the line. This generates a knock-on effect that affects line capacity making it different than the one initially planned in the train schedule defined by the line operator.

The first aspect has been revised in the literature but without a satisfactory solution so far. The majority of works regarding the study of Dwell Times at stations do not consider the uncertainty in them and its effect over line capacity. Although some works look into uncertainty, they do not perform an in-depth analysis of the matter. Medeossi et al. (2011) perform a study using data coming from a real installation with the aim of introducing uncertainty to support a better timetable planning. But the work does not consider the variability of Dwell Times under different service scenarios; they assumed as a valid simplification that the same distributions of Dwell Times could be applied to every scenario.

In San et al. (2016) a revision of the factors affecting Train Dwell times is presented; they conclude that further study of the factors influencing them is required. In Kecman & Goverde (2015) the researchers present a model to predict running times using historical data and apply that to a case study in the Netherlands, but they neglect the impact of variability in Dwell Times related to the time of the day and do not perform a capacity calculation.

Also, Buchmueller et al. (2008) present a model which estimates Dwell Times based on different sub-processes that are evaluated separately to assess their individual influence on Dwell Times; they use real data to quantify it. But they are not considering the influence of passenger volume in their model. In a similar way, Li & Goverde (2016) show a Dwell Time estimation model but without using real passenger demand data. Also, the study does not include an analysis on capacity calculation of the case study that they are presenting.

The second aspect has also been revised in the literature without addressing the aforementioned specificity of Urban Railway lines. A number of works that present models of disturbed railway systems have been published. Just to name a few, in Abril et al. (2008) the authors show simulation methods to reproduce train interactions and knock-on delays. Zhong et al. (2018) show a model to calculate capacity considering disruptions but using random numbers to model the delays.

Also, Huang et al. (2019) present a model based on K-Means clustering capable of analyzing disturbances in real-time operation is presented. The researchers of Zieger et al. (2018) introduce a simulation tool to analyze buffer times by calculating knock-on delays using a Monte-Carlo simulation, but they do not consider realistic delay times but distributions of them. In Goverde et al. (2013) the researchers evaluate capacity consumption under disturbed conditions by means of a Monte-Carlo simulation setup; they apply random distributions of delays to model real operations. The main specificities of urban metro lines are not fully considered, especially the effect of saturation and the generation of subsequent knock-on delays. Although the model

considers hindered movements due to signal aspect restriction, it only uses a part of the minimum headway excluding the approach time while computing the scheduling solution.

The present work shows two different approaches that allow obtaining higher levels of capacity from existing railway installations. The first approach is based on the analysis of uncertain information regarding the capacity calculation. In particular, capacity in urban metro lines is heavily dependent on Dwell Times in the line and therefore it is necessary to analyze its influence on the line capacity estimation. This first approach uses Fuzzy Techniques to model uncertainty regarding Dwell Times in stations.

The aforementioned problem has not been addressed yet in the literature. The proposed models will be especially useful to value the level of saturation of urban railway lines, because the new Fuzzy Maximum Capacity indicators will allow evaluating to what extent the current infrastructure is capable of providing the desired level of transport offer depending on the uncertainty in Dwell Times.

On the other hand, the second approach is based on the analysis of the capacity of the line in disturbed conditions by means of Dynamic Indicators that allow giving additional information which is useful for the infrastructure operators and managers. These Dynamic Indicators are useful to guide capacity improvements by easing the process of deciding among different alternatives of signaling design and redesign in saturated lines. When different scenarios are presented to the infrastructure manager, having the proper tools to choose among them results in a more long-term valuable asset.

1.1. TRANSPORT CAPACITY AND VARIABILITY OF DWELL TIMES IN URBAN RAILWAY LINES

Transport capacity is a vital component of railway systems, defined by the amount of rolling stock per unit of time that the system will be able to move (Dicembre & Ricci, 2011). It depends on multiple factors (Abril et al., 2008; UIC, 2008; Dicembre & Ricci, 2011), such as Infrastructure design, signaling systems, traffic, dwell times at stations and reversing routes at terminus stations.

In suburban lines this capacity calculation is heavily dependent on dwelling times, considering that they suppose an important percentage of the operation time. But these times tend to be variable and uncertain especially during the rush hour. Also, in some situations when there are not real-world data available like in greenfield projects, an approach based on fuzzy modeling proves to be especially convenient to include uncertainty in the model.

In the present work a fuzzy capacity model for railway lines is proposed. Uncertainty in dwell times is introduced by using fuzzy numbers. As a result, new measures of fuzzy

maximum capacity and fuzzy occupancy time rate are proposed. The proposed method provides more information to the railway operator than the standard UIC method that does not include uncertainty regarding dwell times. The model permits as well adjusting the level of fulfillment of the UIC time margins to calculate the operative capacity.

Fuzzy capacity is compared with the operative capacity of a timetable, evaluating if the timetable is feasible under the currently present signaling system design. Fuzzy occupancy time rate is used to calculate the degree of compliance to the UIC robustness reference values. In addition, the model allows calculating the maximum operative capacity that achieves the UIC robustness requirement with a given level of possibility or necessity as a target value.

This approach is considered especially useful in urban railway lines with frequent stops and equipped with automatic driving systems, where the main source of uncertainty is located in dwell times due to passengers getting on and off, and not in running times (Domínguez et al., 2011).

1.2. LINE CAPACITY CALCULATION OF A LINE UNDER DISTURBED TRAFFIC CONDITIONS

The demand for urban transport will increase in 95% until 2050, especially in developing countries where cities are expected to growth hugely in size. Urban dwellers will rise from 4 to 6.4 billion people during the aforementioned period (OECD, 2017).

Railway is one of the most efficient modes of urban public transportation and it has seen an impressive technological improvement during the last few decades. Looking into the future, railway is expected to be a cornerstone to alleviate congestion problems in big cities and metropolis all around the globe.

Specifically, demand for railway urban transport is expected to increase 60% and this rise will put a lot of pressure on current infrastructures. Therefore, city planners and infrastructure managers will have to take complex decisions in order to increase the capacity of current railway networks. Building completely new infrastructures as well as the use of different rolling stock that allow more capacity are options on the table, but they are quite expensive ones. Also, they tend to be constrained by political momentum and funding, the rhythm of which is usually not synchronized with social needs.

But before engaging in lengthy and costly upgrading processes, there are other easier and convenient options that need to be analyzed. Transport capacity limitations in railway networks are caused to a great extent by high dwell times at stations, especially in high density urban lines. These dwell times at stations can be harmful to capacity availability particularly during the rush hour when a great number of

passengers make use of the service. An extended dwell time for a particular train can disrupt the following one, that will have to reduce its speed or even come to a complete stop. This situation happens because the minimum departure-arrival itinerary times required between trains following each other are not fulfilled, and then the following train is too close to the previous one and its movement gets disrupted. So, it becomes key to improve the departure-arrival itinerary times at the station in order to improve the capacity at each of them.

1.3. THESIS OBJECTIVES

1.3.1. MAIN OBJECTIVE

The main objective of this thesis is the development of indicators that allow the improvement of capacity in urban railway lines, considering the main traffic uncertainty triggers, namely dwell times and disturbed traffic conditions.

Furthermore, another main objective of this work is to perform the application of the aforementioned indicators to a real case of application that allows validating the advantages of its use.

1.3.2. SPECIFIC OBJECTIVES

The main specific objective of this thesis is the development of improvement strategies in the design of railway urban infrastructures with the goal of increasing their capacity, in view of the results obtained by using the proposed indicators. The fields of improvement could be railway signaling, strategies for infrastructure design, improvements in railway operation and others.

Specifically:

- Urban Railway lines capacity analysis considering Dwell Times variability. Variability will be modelled by means of Fuzzy Numbers.
- Urban Railway lines capacity calculation in disturbed traffic conditions.
- Development of an Urban Metro simulation model that includes detailed signaling and train movements.
- Test the proposed indicators in a real application case of an urban line close to saturation to assess their validity.

1.4. STRUCTURE OF THE DOCUMENT

This thesis is structured into six chapters:

The first chapter presents an introduction, the motivation, objectives pursued in this thesis and structure of the document.

In the second chapter, the Fuzzy Maximum Capacity and Occupancy Time Rate measurements in urban railway lines are presented. Also, three applications with their resolutions applied to a case study are shown.

The third chapter presents Indicators designed to guide Capacity Improvements in Urban Railway Lines, showing the model, steps necessary for its applications and a case study.

The fourth chapter shows the simulator that has been designed to reproduce accurately the behavior of the urban railway installation used to perform the simulations performed in this work.

The fifth chapter collects the main conclusions obtained from the work presented in the thesis. The most relevant contributions and suggestions for future work are also detailed in this chapter. The sixth chapter shows the papers used as references for the present work.

CHAPTER 2

FUZZY MAXIMUM CAPACITY AND OCCUPANCY TIME RATE MEASUREMENTS IN URBAN RAILWAY LINES

2.1. INTRODUCTION

Nowadays, many of the urban railway lines are severely congested, especially during rush hour. This is due partially to the great population growth that cities have experimented, especially the larger ones, during the latest years. In 1950, only 30% of the population lived in cities while at the present time this figure has increased to 54% and it is expected to reach 66% by 2050 (United Nations, 2014).

Therefore, on the one hand operators and managers of railway infrastructures are facing the challenge of increasing the available capacity at existing installations to cover the expected growth of demand. On the other hand, the operation of installations under conditions close to saturation is prone to be unstable, because the minimum incident causes a chain of delays down the line that affect negatively the service quality and the overall service reliability offered by the system.

Transport capacity is a vital component of railway systems. In fact, it is the product that infrastructure managers offer to the market as well as a measurement representing the amount of rolling stock per unit of time that the system will be able to move (Dicembre & Ricci, 2011).

Even though the concept of capacity is intuitive, its technical quantification in order to make it useful in the evaluation and proper design of railway infrastructures is complex. This has led to the definition of different types of capacity in the literature (Krueger, 1999; Abril et al., 2008; Kontaxi & Ricci, 2010; Ortega et al., 2015).

- **Theoretical or maximum capacity**: Maximum volume of traffic usually expressed as number of trains per hour that can travel through a railway network or network section without the circulation of the trains being affected by the signaling systems. This in practice means that trains should not brake due to the proximity to another previous train circulating that could force them to slow down or to increase their dwell time at stations.

  Under this scenario, the signaling system always allows trains to move at the maximum speed allowed at every point of the line, always considering the existing safety configurations.

- **Practical capacity**: Volume of traffic that can travel through the system permanently maintaining a reasonable quality of service. It is a value smaller than theoretical capacity, because buffer margins between circulations are required to avoid small delays being transmitted to other trains (Salido & Tarazona, 2008; Hansen, 2009; Dicembre & Ricci, 2011), therefore that reduces the number of trains in circulation with respect to theoretical capacity which does not apply this buffer margin.

  Typically, practical capacity is calculated as a percentage of theoretical capacity (between 60 and 85%), depending on the type of use (UIC, 2013). This measurement of capacity turns out to be more useful to infrastructure managers, considering that it is related to the real capacity they can offer because it considers the true operating conditions in the installation.

- **Operative Capacity used by a timetable**: it is the volume of traffic contained in a timetable for a period of time. In order to make that timetable operative under an acceptable level of service quality, the value has to be inferior to the practical capacity. It offers a measurement of the infrastructure level of use and, therefore, of its saturation level. It can be expressed as a percentage of use regarding the maximum capacity; therefore, it gives information about the infrastructure level of occupation.

- **Available capacity**: difference between the practical capacity and the operative capacity. It offers information about the residual capacity of a timetable.

Transport capacity depends on multiple factors, (Abril et al., 2008; UIC, 2008; Dicembre & Ricci, 2011), such as:

- **Infrastructure design**: Defined by track topology, gradients and speed limitations present in the system.

- **Trains specifications**: They determine their performance figures such as acceleration rate, maximum speed and braking force. These parameters limit the distance allowed between two consecutive circulating trains while the required safety level is maintained.

- **Signaling systems**: They are in charge of guaranteeing train movements and keeping them at enough distance from one another. In urban lines signaling systems typically use fixed blocks, which implies having signals that inform the driver placed on the border between blocks. They give the driver information about what is beyond his field of vision. Train detection on track is performed using either axle-counter systems or track circuits, which make possible

determining the block or blocks being occupied by the train at all times. Therefore, resolution regarding train location is limited by the length of track blocks and this in turn limits the capacity the system is capable of offering. Likewise, in installations with an ATP speed codes safety system the maximum designed speeds for every block imply another restriction. And the line design itself, with its associated itineraries and stops, limits the maximum capacity the line can offer.

In addition to this typical configuration, there are systems like the ones based on CBTC that allow a more precise train location with the use of continuous bidirectional communication between train and track equipment. This increases system resolution and consequently its available capacity, as trains can run closer in the line.

Also, Automatic Train Operation (ATO) systems may introduce an additional limitation to the capacity offered by the system while prioritizing other aspects like comfort or energy efficiency.

And the Centralized Traffic Control (CTC), which is in charge of centralizing the control of the interlockings and traffic flows of the line, similarly influences system capacity by enabling the automatic dispatching of routes, following predefined operation strategies.

- **Traffic**: which is defined as the mix of trains, train sequences and priority rules at railway nodes. Capacity is reduced when trains with different speeds or lengths travel one after another, or under a different dwelling schedule (Burdett & Kozan, 2006). All the previous situations are possible in railway urban lines. Typically, cyclical timetables are defined for every period of demand in Metro lines: peak or off-peak hours. These timetables define a predefined sequence of trains, priority rules at nodes and a commercial dwelling schedule, usually with constant frequencies for every type of service. This traffic structure forms a cyclical pattern in which capacity calculation depends heavily. The maximum capacity of an infrastructure is often identified with its capacity during the peak hour by analyzing the period of its traffic pattern.

- **Dwell Times at stations**: They have a great influence on capacity and are affected by door opening and closing times as well as time waiting to depart once the doors close, passenger flow time and time the doors remain open after passenger flow ceases (Kittelson & Associates et al.,2013). The required times to allow the passengers getting in and off at train stops have a great

influence on capacity, especially in metro lines where they are very common as well as during peak hours when there is a high frequency of trains and passengers in the line. Also, Dwell Times in these lines are subject to fluctuations owed to variable passenger traffic as much as to its own process of loading and unloading trains and its associated procedure for doors closing, which is performed manually by the driver in many lines. Therefore, uncertainty in commercial Dwell Times is a key problem in the calculation of capacity in metro lines.

- **Reversing routes at terminus stations**: Terminus stations are the ones located at every end of the railway line; in them all trains leave in the reverse direction from that of their arrival. They tend to be critical nodes and therefore the way trains are reversed in them conditions capacity of whole line as well. In this procedure, both signaling system involved and operative time associated have influence, as well as the time required by the driver to change cabin or being replaced by a coworker.

In regard to capacity calculation, there are analytical methods that allow obtaining a theoretical capacity value in a relatively simple manner by using mathematical expressions applied to simplified models of the system, to which a certain margin has been applied to approximate the practical capacity really obtained in the installation.

One of the most well-known is the one proposed by the International Union of Railways (UIC, 1996) in its 405 leaflet, which is applied to the critical section of the line and defines capacity as:

$$P = \frac{T}{t_{fm} + t_r + t_{zu}} \qquad (2\text{-}1)$$

Where:

T: time of reference
t_{fm}: minimum time between consecutive trains
t_r: buffer time to allow a certain level of service quality
t_{zu}: time required because of the blocks design of the line.

Other subsequent methods are based on this concept, like the one proposed in Robert et al. (2006) which uses the proportions of types of trains in the system as well as their direction and percentage flows in the nodes as static values of the system.

De Kort et al. (2003) present a method of capacity analysis that uses blocks which represent elements of the system. It analyzes different topologies of track layout and signaling systems, allowing quantifying how they influence system capacity.

Even though analytical methods are based on real-world data of infrastructure and

timetables, they are only useful as a starting point in simple situations where the use of more complex techniques can be avoided because there is no need to achieve a more precise result. In addition, they could be used to detect installation bottlenecks.

There are some works that have made comparisons between some analytical methods, like for example Malavasi et al. (2014), but in general the suitability of each one of them will depend on the specific application case.

Analytical methods are not useful to precise the behavior during the interactions and conflicts between trains, which is something basic to analyze complex railway lines with high circulation intensity, like is the case regarding urban ones.

On the other hand, there are calculation methods based on the widely known as timetable compression method. For example, UIC proposes in (UIC, 2013) their reference method of capacity calculation UIC 406R. It aims to establish an international standard to evaluate capacity in different environments by establishing a common framework and uniform principles.

The method is based on real installation timetables and the undisturbed space-time movement of the trains, which is defined in the circulations timetable. The circulations order, passing order at nodes and halts schedule all get fixed beforehand; that forms the traffic pattern of the line. The method performs a compression of the pattern of traffic by bringing the trains closer to the limit allowed by the signaling system without their circulation being affected and keeping their dwelling times for passengers loading and unloading constant. Figure 2-1 shows an example of its application.

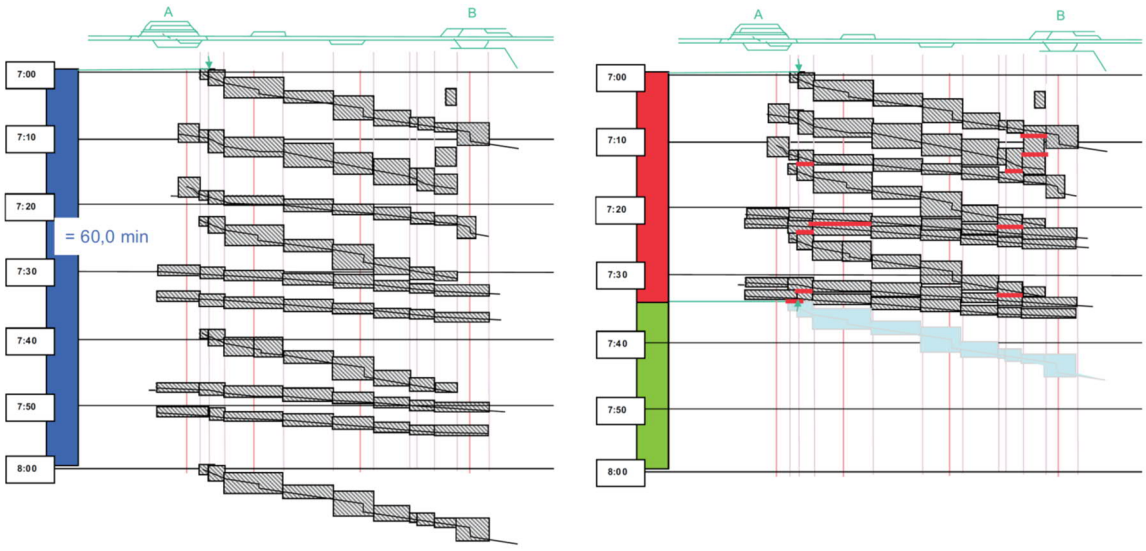

Figure 2-1. Left: Original timetable. Right: Compressed timetable (UIC 406R)

That is to say, the compression method eliminates buffer times between trains, calculating the maximum capacity as the number of trains per hour contained in the timetable within the compressed time. The margin reaches zero in the critical point that limits capacity.

By comparing the real timetable with the compressed one, the occupancy time rate measure of a given timetable is defined as the compressed time divided by the timetable time window. This value can be compared to the reference values proposed by the UIC for various types of railway lines (Table 2-1).

Type of line	Peak Hour	Daily Period
Dedicated suburban passenger traffic	85%	70%
Dedicated high-speed line	75%	60%
Mixed-traffic lines	75%	60%

Table 2-1. Proposed occupancy time rate values

This allows checking the margin of capacity still available within the system. If the occupancy time rate is not yet over the recommended values, the timetable generally allows adding more circulations if that is required, before recalculating again the occupancy time rate. When the reference value is surpassed, the timetable is already saturated and does not allow adding any more circulations. The occupancy time rate values recommended by the UIC for suburban traffic are 85% during peak hours and 70% on daily period.

In suburban lines this capacity calculation is heavily dependent on dwelling times, considering that they suppose an important percentage of the compressed time. For example, in the Barcelona-Vallès line of the Spanish operator FGC they suppose up to 20% during peak hours. However, the compression method does not include the uncertainty associated to dwelling times, which are modelled as being constant, and therefore does not allow analyzing the effect of their variability in the obtained capacity value.

An effective procedure to calculate the compressed time and the maximum capacity is the use of simulation models that allow reproducing the full railway system at a micro level by using tools like OpenTrack or MultiRail. By means of them, it is possible to calculate the maximum capacity of a railway system using the compression method. This is accomplished by approximating the trains until they could not get closer without affecting each other; that is the conflict-free compressed time.

Some works present their own simulation tool (Ballis et al., 2004; Goverde et al., 2013). Goverde et al. (2013) presents an example of capacity consumption calculation method that uses the compression method. It adds uncertainty by means of Weibull distributions that allow randomizing line entry times, but dwelling times are considered fixed.

On the other hand, Landex (2012) shows a tool that calculates capacity measured as an average of Scheduled Waiting Times (SWT) in a sample of possible timetables of a certain infrastructure. The system does not require a defined timetable, just the number, order and type of trains and infrastructure design. Then, and based on this setup, a large number of timetables are defined and their SWT are obtained. The timetable with the lowest SWT that fulfills the capacity requirements may be chosen.

As aforementioned, the capacity of a system is conditioned by its traffic pattern. There are studies centered in finding traffic patterns that offer the largest capacity. In Ortega et al. (2015) some optimization models developed by other authors (Jovanovic & Harker, 1991; Carey, 1994; Higgins et al., 1996; Caprara, 2002) are mentioned. Jovanovic & Harker (1991) show an optimization tool aimed to assess the feasibility of a given schedule, which searches over different possible plans and tries to find if at least one of them could accomplish the expected schedule. The algorithm employed to solve the problem is a branch-and-bound implementation. Higgins et al. (1996) demonstrate an optimization single-track scheduling model, also based in branch-and-bound.

In Carey (1994) a mathematical model for train pathing and some heuristic techniques that allow reducing its required computing load are exposed. These are typical strategies commonly followed by experienced human dispatchers.

As for Caprara (2002), the author presents a method based on directed multigraphs to solve the timetabling problem. The resulting linear programming model is solved by means of Lagrangian relaxation, which decreases the problem-solving time.

Mussone & Wolfler (2013) propose a different approach to capacity calculation based on an optimization method. The system is modelled using inequalities. These constraints due to the probability of interference between trains are non-linear, then so is the system. An iterative approach through constraints relaxation is applied until the solution converges to a definite solution.

As mentioned before, capacity in urban railway systems depends heavily on stops made by trains at station platforms, resulting in a higher system capacity when the dwelling times are shorter. The major part of performed works about capacity does not consider uncertainty related to dwelling times, although there are some exceptions.

In Medeossi et al. (2011), Dwell Time variability is considered by gathering real-world data and using it to simulate separate train courses many times to obtain their time-distance diagram represented as a cluster of dots. Where the different diagrams for each train collide, there is a probability of conflict. A revision of deterministic models about dwelling times is performed in San et al. (2016). They all gather real-world data from several installations, the work concludes that the number of passengers getting on and off and waiting at platforms are the most influencing parameters.

In Kecman & Goverde (2015) real global and local data of the studied corridor are used and a robust linear regression, regressions trees and random forests. It concludes that dwell times, although heavily correlated to arrival delays for the case of on time trains, cannot be fully explained by means of the selected predictor variables.

Buchmueller et al. (2008) in turn divide dwell time into five subprocesses: door unblocking, opening and closing, passenger boarding and alighting and train dispatching. They present a statistical analysis using real passenger data for every station and type of train, but without considering the number of passengers present on each wagon.

On the contrary, Li & Goverde (2016) show a dwell time estimation model without the use of passenger real data. It uses instead other predictors, being the one relatively most accurate the dwell time at the previous station with a correlation coefficient of 0,456.

Some of the works in the literature are completely centered on the study of passenger influence on dwelling times. In Jiang et al. (2015) a simulation model of dwelling times that was generated by using real data coming from Shanghai Metro is presented. It is based on the passenger boarding and alighting times and delays caused by overcrowded vehicles preventing door closing on the first attempt. Another similar approximation to the study of dwell times is proposed in Perkins et al. (2014) which developed a mesoscopic passenger simulation model. Zhang et al. (2008) present a cellular automata-based alighting and boarding passenger model that considers their individual and group behavior.

Chu et al. (2015) propose an approximation to the problem by a feedforward neural network that is compared to an own microsimulation model, demonstrating that the first one fits better to real-world obtained data.

In some situations, there are not real-world data available. This is the case of greenfield projects where no previous information is available or when the timetables of a line need to be modified. In both cases, the previous statistical data of the line are not completely useful any longer, as these modifications invalidate the previous existing information regarding delays. In this situation, an approach based on fuzzy modeling proves to be especially convenient to include uncertainty in the model.

The modelling of uncertainty by means of fuzzy knowledge (Bellman & Zadeh, 1970) has been extensively used in the literature for different applications. In Chan & Thia (1996) they present a fuzzy expert system aimed to perform the online rescheduling of mass transit rapid systems by managing train dwelling times at stations. It defines as fuzzy sets line regularity, risk and congestion. Chanas & Kasperski (2001) use fuzzy logic and hybrid genetic algorithms to minimize maximum lateness of a machine solving a scheduling problem. Balaji (2011) present a type-2 fuzzy logic based urban management traffic system.

In Cucala et al. (2012) delays at the departure station are modeled using fuzzy numbers in order to optimize the timetable of a train subject to punctuality restrictions. Milinković et al. (2013) propose to use expert knowledge to define rules and fuzzy sets that allow obtaining a calculation model for primary and secondary delays based on a fuzzy Petri net.

Also, there are some works related to timetables, for example in Yang et al. (2009) a model is proposed to solve the timetable planning of a line by applying fuzzy information on passenger demand. The optimum solution is obtained through the application of a branch and bound algorithm. In an analogous manner, Isaai et al. (2011) propose a model to obtain the best trains timetable by using fuzzy AHP, a methodology

of alternatives selection based on fuzzy set theory and hierarchical structure analysis and with the goal of obtaining the best possible timetable via the aggregation of multiple service performance figures.

In Fay (2000) a dispatching support system for railway operation control is described, it uses Petri Nets and Fuzzy Sets to model rule-based expert knowledge. In the previous works the use of fuzzy numbers has proven its utility to model uncertainty in passenger attendance to stations or other parameters related to scheduling and railway traffic management. However, this modeling technique has not yet been applied to fuzzy capacity calculation in a greenfield project, a redesign of an existing infrastructure or a timetable modification. Typically, in these situations statistical data regarding dwelling times are not available.

In the present work a fuzzy capacity model for railway lines is proposed. Uncertainty in dwell times is introduced by using fuzzy numbers. As a result, new measures of fuzzy maximum capacity and fuzzy occupancy time rate are proposed. The proposed method provides more information to the railway operator than the standard UIC method that does not include uncertainty regarding dwell times. The model permits as well adjusting the level of fulfillment of the UIC time margins to calculate the operative capacity.

Fuzzy capacity is compared with the operative capacity of a timetable, evaluating if the timetable is feasible under the current signaling system design. Fuzzy occupancy time rate is used to calculate the degree of compliance to the UIC robustness reference values. In addition, the model allows calculating the maximum operative capacity that achieves the UIC robustness requirement with a given level of possibility or necessity as a target value.

This approach is considered especially useful in urban railway lines with frequent stops and equipped with automatic driving systems, where the main source of uncertainty is located in dwell times due to passengers getting on and off, and not in running times (Domínguez et al., 2011). It provides valuable information regarding results robustness in comparison to other models using deterministic stopping times.

In table 2-2 a summary showing the different references found in the literature is presented. It offers also information regarding their specific use in an urban lines application.

	Urban Lines	Notes	Reference
Own Tool	✓	No Uncertainty	(Ballis et al., 2004)
	✗	Uncertainty with Weibull	(Goverde et al., 2013)
	✗	Cap. Calculation own tool	(Landex, 2012)
	✗	Schedule viability optimization (B&B)	(Jovanovic & Harker, 1991)
	✗	Single-track optimization (B&B)	(Higgins et al., 1996)
	✗	Multigraphs to solve timetabling problem	(Caprara, 2002)
	✗	Calculation based on optimization	(Mussone & Wolfler, 2013)
Dwell Times	✗	Simulates different train courses	(Medeossi et al., 2011)
	✗	Real-world data	(San et al., 2016)
	✗	Not fully explained by predictor variables	(Kecman & Goverde, 2015)
	✗	5 subprocesses, pax not considered	(Buchmueller et al., 2008)
	✗	Estimates with DT at previous station	(Li & Goverde, 2016)
	✓	Simulates pax process. Uses real data, no uncertain.	(Jiang et al., 2015)
	✗	Mesoscopic pax simulation	(Perkins et al., 2014)
	✓	Cellular automata pax model, No Capacity calcul.	(Zhang et al., 2008)
	✓	Feedforward Neural Network pax model. No Capac.	(Chu et al., 2015)
Fuzzy	✓	Expert system Dwell Times managing. No capacity.	(Chang & Thia, 1996)
	✗	Machine solving a scheduling problem	(Chanas & Kasperski, 2001)
	✓	Type-2 logic urban management traffic system	(Balaji, 2011)
	✗	Delays modeled to optimize timetable	(Cucala et al., 2012)
	✓	Calculation model for delays. Petri net, no capacity.	(Milinković et al., 2013)
	✗	Timetable planning using info on pax demand	(Yang et al., 2009)
	✗	Best timetable by using fuzzy AHP	(Isaai et al., 2011)
	✗	Dispatching system. Petri Nets + Fuzzy Sets	(Fay, 2000)

Table 2-2. State of the art – Summary table

The proposed model is applied to a real case in a section of the Vallès line of the Catalan operator FGC, which is currently saturated and under study to be partially redesigned. A railway traffic simulator based on OpenTrack has been configured and used to apply the UIC timetable compression method.

2.2. FUZZY CAPACITY MODEL

2.2.1. MODEL DESCRIPTION

In this section, a model to calculate maximum capacity and occupancy time rate measurements using fuzzy numbers is proposed. This allows considering uncertainty regarding dwell times at platforms in urban railway lines and analyzing capacity dependency in relation to those times. To that effect, the compression method defined in UIC (2013) is applied. The compression method is a generalized method for calculating capacity consumption section by section. An example of its application is shown in Figure 2-2; the left figure shows 11 consecutive train paths departing from Gràcia station with destination Sarrià. The T_{ope} is reflecting the cycle time of 2 trains following a certain timetable.

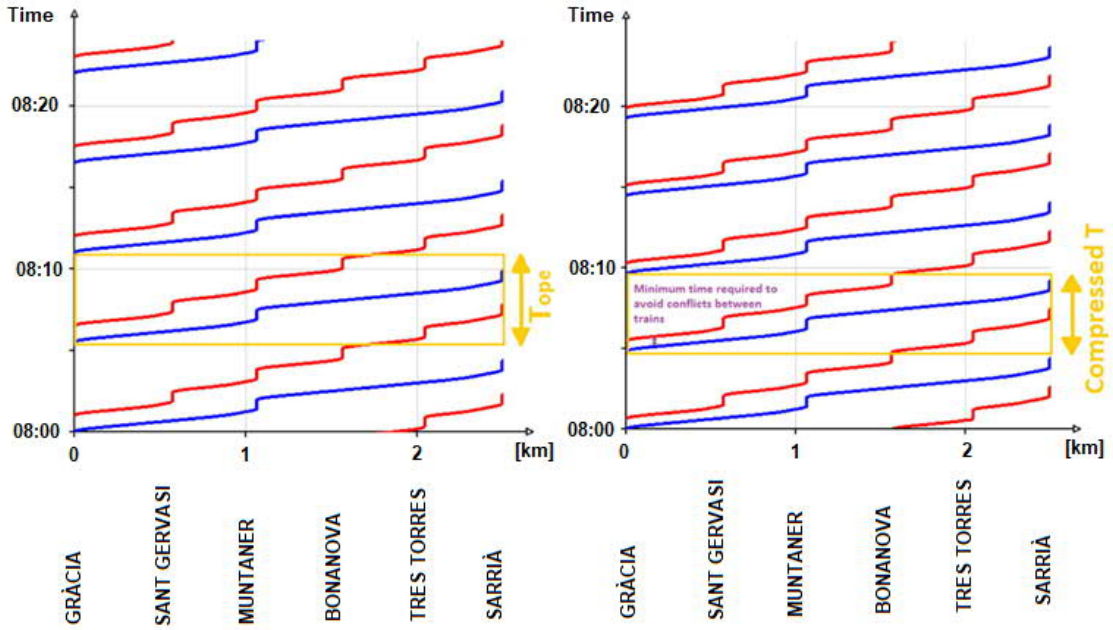

Figure 2-2. Train paths diagram and the timetable compression method (Left: Uncompressed paths from the schedule. T_{ope} reflects the periodic cycle time of 2 trains, Right: Compressed paths)

The diagram on the right in Figure 2-2 shows the same train paths but compressed until trains cannot get any closer without affecting each other, therefore eliminating buffer time margins between trains.

Given a periodic traffic pattern that determines the sequence of trains in the cycle and a signaling and operation system the maximum line capacity is calculated as:

$$C = \frac{3600 \cdot n}{T} \qquad (2\text{-}2)$$

Where:

T: conflict-free compressed time in seconds of the traffic pattern, according to UIC

n: number of trains circulating in the pattern

Therefore, the capacity C is measured in trains per hour. After setting the traffic pattern,

the compressed time T can be expressed as a function of dwell times in the stations of the analyzed line section:

$$T = \mathrm{f}(T_{\mathrm{Dk}}) \qquad (2\text{-}3)$$

Where:

k = 1, 2…S

Where T_{Dk} is the dwell time at each platform k, and S is the number of stops. Function f will be calculated in the case study by using a detailed traffic, signaling and control systems simulator.

$$\mathrm{C} = \frac{3600 \cdot n}{\mathrm{f}(T_{\mathrm{Dk}})} \qquad (2\text{-}4)$$

The uncertainty associated to dwell times can be modeled as fuzzy numbers $\tilde{T}_{Dk}$, and thus, the obtained compressed time is as well a fuzzy number:

$$\tilde{T} = \mathrm{f}\left(\tilde{T}_{\mathrm{Dk}}\right) \qquad (2\text{-}5)$$

Where k = 1, 2…S

In this way, the proposed Fuzzy Maximum Capacity (see equation 2-6) is a function of the fuzzy dwell times:

$$\tilde{C} = \frac{3600 \cdot n}{\mathrm{f}(\tilde{T}_{\mathrm{Dk}})} = \mathrm{F}(\tilde{T}_{\mathrm{Dk}}) \qquad (2\text{-}6)$$

The function f increases with Dwell Times. Hence, the maximum capacity decreases with those times. Thus, it is possible to easily calculate the fuzzy maximum capacity $\tilde{\mathrm{C}}$ by means of α-cut arithmetic (Chanas et al., 1984).

The upper limit of each α-cut of the fuzzy $\tilde{\mathrm{C}}$ ($\mathrm{C}^{\overline{\alpha}}$) can be obtained considering the lower limit of the α-cut of the fuzzy $\tilde{\mathrm{T}}_{\mathrm{Dk}}$ ($\mathrm{Td}^{\underline{\alpha}}$) (see equation 2-7 and Figure 2-2). Similarly, the lower limit of each $\tilde{\mathrm{C}}$ α-cut ($\mathrm{C}^{\underline{\alpha}}$) can be obtained using the upper limit of the $\tilde{\mathrm{T}}_{\mathrm{Dk}}$ α-cut ($\mathrm{Td}^{\overline{\alpha}}$) (see equation 2-8 and Figure 2-3). This way, by varying the α value between 0 and 1, the whole $\tilde{\mathrm{C}}$ set can be obtained.

$$C^{\overline{\alpha}} = \mathrm{F}(\mathrm{Td}^{\underline{\alpha}}) \qquad (2\text{-}7)$$

$$C^{\underline{\alpha}} = \mathrm{F}\left(\mathrm{Td}^{\overline{\alpha}}\right) \qquad (2\text{-}8)$$

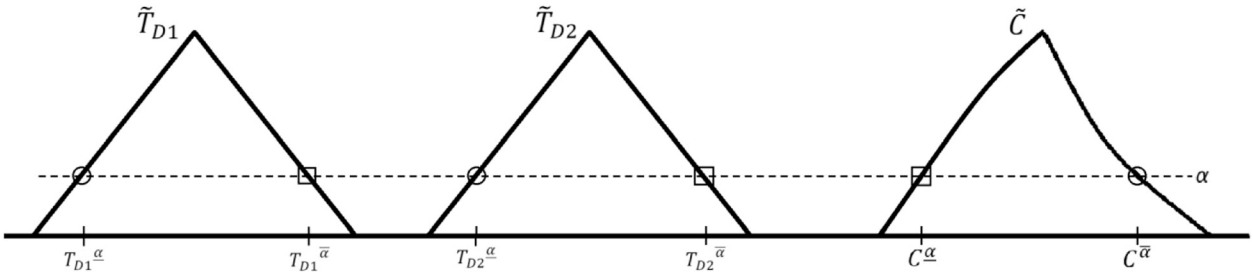

Figure 2-3. Fuzzy capacity obtained from fuzzy Dwell Times

Given the fuzzy maximum capacity, and a timetable with an associated operative capacity C_{ope}, the Fuzzy Occupancy Time Rate $\widetilde{U}$ can be defined as:

$$\widetilde{U} = \frac{C_{ope}}{\tilde{C}} \cdot 100 \qquad (2\text{-}9)$$

2.2.2. RAILWAY TRAFFIC OPERATOR APPLICATIONS

Using the previous model definitions of $\tilde{C}$ and $\widetilde{U}$, three practical problems from the perspective of the railway traffic operator could be set out:

- Is the operative capacity achievable?
- Does the operative capacity keep enough reliability margins?
- Calculation of the highest C_{ope} that fulfills the recommended UIC Occupancy Time margins with a target possibility/necessity value

These three applications are described and solved in the following subsections.

2.2.2.1. FIRST APPLICATION: IS THE OPERATIVE CAPACITY ACHIEVABLE?

Given a timetable, the first question is to determine if the associated operative capacity C_{ope} is below the Fuzzy Maximum Capacity, to assess if the timetable is feasible under the current signaling system (see equation 2-10):

$$C_{ope} \leq \tilde{C} \qquad (2\text{-}10)$$

The advantage of using the fuzzy value comparison instead of the crisp one is that the inherent uncertainty of dwell times is properly considered. The fuzzy number $\tilde{C}$ is compared to the crisp number C_{ope} in terms of possibility Π and necessity N measures (Dubois & Prade, 1983), providing the possibility and the necessity that the C_{ope} is below the fuzzy maximum capacity (equations 2-11 and 2-12). Thus, Railway operators obtain more information about the degree of fulfillment of the maximum capacity.

$$\Pi(\tilde{C} \geq C_{ope}) \quad (2\text{-}11)$$

$$\mathrm{N}(\tilde{C} \geq C_{ope}) = 1 - \Pi(\tilde{C} < C_{ope}) \quad (2\text{-}12)$$

Two examples are presented below:

In Figure 2-4, the possibility of $\tilde{C}$ being greater than or equal to C_{ope} is α, and the necessity of $\tilde{C}$ being greater than or equal to C_{ope} is zero, since:

$$\mathrm{N}\left(\tilde{C} \geq C_{ope}\right) = 1 - \Pi\left(\tilde{C} < C_{ope}\right) = 1 - 1 = 0 \quad (2\text{-}13)$$

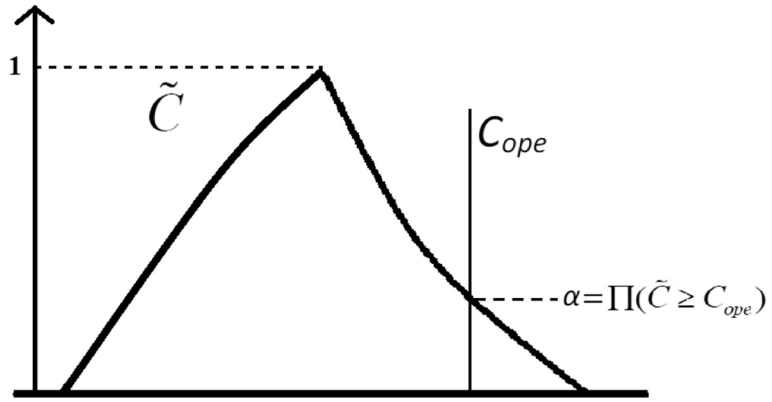

Figure 2-4. Fuzzy maximum capacity compared to Operative Capacity C_{ope} at the right side

In Figure 2-5, the possibility of $\tilde{C}$ being greater than or equal to C_{ope} equals to 1, and the necessity of $\tilde{C}$ being greater than or equal to C_{ope} equals to 1 – α, since:

$$\mathrm{N}\left(\tilde{C} \geq C_{ope}\right) = 1 - \Pi\left(\tilde{C} < C_{ope}\right) = 1 - \alpha \quad (2\text{-}14)$$

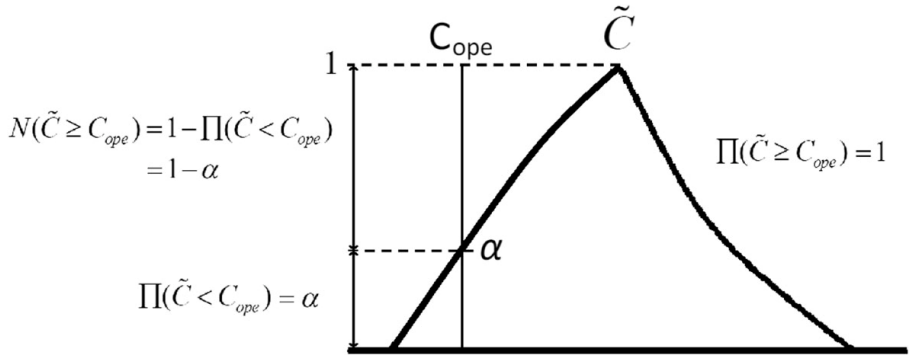

Figure 2-5. Fuzzy maximum capacity compared to Operative Capacity, C_{ope} at the left side

2.2.2.2. SECOND APPLICATION: DOES THE OPERATIVE CAPACITY KEEP ENOUGH RELIABILITY MARGINS?

In the first application it has been checked if the Operative Capacity is less than the Theoretical Fuzzy Maximum Capacity. But this condition does not ensure that a timetable is robust enough to incidents in the line. To conclude that a timetable allows an operation that is reliable, which means that it can compensate delays by using enough time buffer margins, the timetable needs to preserve certain occupancy time rate reference values (UIC, 2013). The fuzzy occupancy time rate is calculated for a given timetable, as its associated operative capacity divided by the fuzzy maximum capacity (in %) (equation 2-9).

Therefore, the Fuzzy Occupancy Time Rate of the line can be compared to the reference values proposed by the UIC:

$$\widetilde{U} \leq U_{UIC} \quad (2\text{-}15)$$

$$\frac{C_{\mathrm{ope}}}{\tilde{C}} 100 \leq U_{\mathrm{UIC}} \quad (2\text{-}16)$$

$$\frac{C_{\mathrm{ope}}}{U_{\mathrm{UIC}}} 100 \leq \tilde{C} \quad (2\text{-}17)$$

Where U_{UIC} is the maximum occupancy time rate reference value recommended by the UIC. This value is defined for every type of railway line and service hour (Table 2-1).

The degree of compliance to the UIC robustness requisite is evaluated again in terms of possibility and necessity measures, but this time comparing the fuzzy maximum capacity $\tilde{\mathrm{C}}$ to the proportion of the operative capacity $\mathrm{C_{ope}}$ over the UIC reference value $\mathrm{U_{UIC}}$ (equation 2-17). Again, railway operators obtain information about the degree of fulfillment of the UIC recommended occupancy time rate values. Then, possibility and necessity measures associated with the fuzzy comparison are calculated with a procedure akin to the one described previously in the first application.

2.2.2.3. THIRD APPLICATION: CALCULATION OF THE HIGHEST C_{OPE} THAT FULFILLS THE RECOMMENDED UIC OCCUPANCY TIME MARGINS WITH A TARGET POSSIBILITY/NECESSITY VALUE

Finally, once the fuzzy maximum capacity associated with an infrastructure and a certain traffic pattern has been calculated (taking into account the uncertainty in dwell times), the proposed model allows calculating the maximum operative capacity C_{ope} that achieves the UIC robustness requirement with a given level of possibility or necessity as a target. To that effect, the C_{ope} of the following equations has to be calculated depending if the imposed requirement is a possibility value α_{obj} of a necessity value $\mathrm{N_{obj}}$:

$$\prod\left(\frac{C_{\mathrm{ope}}}{U_{\mathrm{UIC}}} 100 \leq \tilde{C}\right) = \alpha_{\mathrm{obj}} \quad (2\text{-}18)$$

$$\mathrm{N}\left(\frac{C_{\mathrm{ope}}}{U_{\mathrm{UIC}}}100 \leq \tilde{C}\right) = N_{\mathrm{obj}} \qquad (2\text{-}19)$$

Where α_{obj} and $\mathrm{N}_{\mathrm{obj}}$ are the target levels of possibility and necessity that could be imposed as the level of fulfillment of the UIC recommended value.

2.3. MODEL RESOLUTION

In this section the procedure to solve the problems laid out in the previous section is described.

2.3.1. PROBLEMS 1 AND 2 RESOLUTION

A procedure to solve problems 1 and 2 without the need of generating the whole $\tilde{C}$ number, which would require repeated iterations, is proposed. This procedure is based on the alpha-cuts arithmetic (see Figure 2-3). The method for the first problem is the following:

- For α equal to 0, the simulation function $F(T_{Dk})$ is applied using the ${T_{Dk}}^{\underline{\alpha}}$ values. The resulting capacity value is the upper limit of the α-cut of $C^{\overline{\alpha}}$ with α equal to 0 (see Figure 2-6). If this $C^{\overline{\alpha}}$ value is lower than C_{ope}, the possibility and necessity of $C_{ope} \leq \tilde{C}$ are null and the algorithm ends.

- For α equal to 0, the simulation function $F(T_{Dk})$ is applied using the ${T_{Dk}}^{\overline{\alpha}}$ values. The resulting capacity value is the lower limit of the α-cut of $C^{\underline{\alpha}}$ with α equal to 0 (see Figure 2-6). If this $C^{\underline{\alpha}}$ value is higher than C_{ope}, the possibility and necessity of $C_{ope} \leq \tilde{C}$ are equal to 1 and the algorithm ends.

- For α equal to 1, the simulation function $F(T_{Dk})$ is applied using the ${T_{Dk}}^{\overline{\alpha}} = {T_{Dk}}^{\underline{\alpha}}$ values, that is, the core of the triangular fuzzy numbers. The resulting capacity value is the core of the fuzzy maximum capacity (α equal to 1) (see Figure 2-6).

- If C_{ope} is higher than $C^{\overline{\alpha}} = C^{\underline{\alpha}}$ with α equal to 1, then the cutting point between C_{ope} and $\tilde{C}$ has to be found in the upper limits of the α-cuts of $\tilde{C}$ by using the bipartition method simulating $F(T_{Dk})$ with the lower limits of $\tilde{T}_{Dk}$ α-cuts. In this situation, the necessity value is null, and the possibility value is calculated as the α value of the cutting point (see Figure 2-4), and the algorithm ends.

- If C_{ope} is lower than $C^{\overline{\alpha}} = C^{\underline{\alpha}}$ with α equal to 1, then the cutting point between C_{ope} and $\tilde{C}$ has to be found in the lower limits of the α-cuts of $\tilde{C}$ by using the bipartition method simulating $F(T_{Dk})$ with the upper limits of $\tilde{T}_{Dk}$ α-cuts. In this situation, the possibility value equals to 1 and the necessity value is calculated as 1 minus the α value in the cutting point (see Figure 2-5), and the algorithm ends.

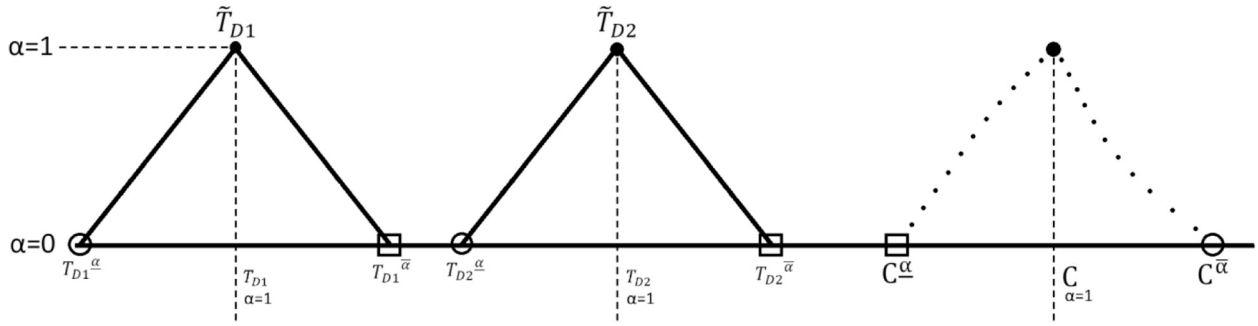

Figure 2-6. Calculation of the core and the support of fuzzy maximum capacity obtained from triangular fuzzy Dwell Times, α-cuts method.

If the fuzzy $\tilde{\mathrm{T}}_{\mathrm{Dk}}$ numbers representing dwell times have a core longer than 0 (for example trapezoidal fuzzy numbers), the same procedure can be applied.
The same procedure can be used to solve problem number 2, considering that in problem 2 the fuzzy maximum capacity $\tilde{\mathrm{C}}$ has to be compared to $\frac{C_{\mathrm{ope}}}{U_{\mathrm{UIC}}}100$ (that is a crisp value) instead of C_{ope}.

2.3.2. PROBLEM 3 RESOLUTION

To calculate the limit C_{ope} of the timetable that fulfills the UIC reference value with a target possibility α_{obj} (thus, the associated necessity value is 0), C_{ope} can be isolated out of the following equation:

$$\prod\left(\frac{C_{\mathrm{ope}}}{U_{\mathrm{UIC}}}100 \leq \tilde{C}\right) = \alpha_{\mathrm{obj}} \qquad (2\text{-}20)$$

To this end, $C^{\overline{\alpha}}$ has to be calculated with α equal to α_{obj} (see Figure 2-4), that is, just one simulation is required $F(T_{Dk}{}^{\underline{\alpha}})$ with α equal to α_{obj}. Finally, the C_{ope} that meets the specified requirement is obtained as the result of multiplying $C^{\overline{\alpha_{obj}}}$ by $U_{UIC}/100$.

If the accomplishment of a certain level of necessity N_{obj} is fixed as a goal (thus, the associated possibility value is 1), C_{ope} can be calculated from the equation:

$$\mathrm{N}\left(\frac{C_{\mathrm{ope}}}{U_{\mathrm{UIC}}}100 \leq \tilde{C}\right) = N_{\mathrm{obj}} \qquad (2\text{-}21)$$

For this purpose, $C^{\underline{\alpha}}$ has to be calculated (see Figure 2-5) with α equal to 1 minus N_{obj}, that is, just one simulation is required $F(Td_{Dk}{}^{\overline{\alpha}})$ with α equal to 1 minus N_{obj}. Finally, the C_{ope} value that meets the specified requirement is obtained as the result of multiplying $C^{\underline{\alpha}}$ by $U_{UIC}/100$.

2.4. CASE STUDY

A section of the FGC Barcelona-Vallès network has been chosen to apply the proposed model. FGC (Ferrocarrils de la Generalitat de Catalunya) is a railway company that operates several lines in Catalonia, a region located at the northeast of Spain.

The Barcelona-Vallès infrastructure (line map in Figure 2-7) is equipped with a safety system called ATP (Automatic Train Protection), which is in charge of supervising the train speed and applying the penalty brake in the event of safety conditions not being fulfilled. This line is equipped with a speed codes implementation scaled to 90/60/45/30/0 kilometers per hour.

Figure 2-7. Map of FGC Barcelona-Vallès lines

The section Gràcia-Sarrià covers one of the most congested parts of the network, comprising the nodes of Gràcia and Sarrià, which are two key points of the whole network. The first one is the main node serving several lines: L6, L7, S1, S2, S5 and S55.

With the aim of obtaining precise times of the itineraries in the installation, a parametric model of the section has been implemented using a simulation tool. This tool allows modelling line profile data and track topology as well as rolling stock and the routes for each interlocking of the line.

2.4.1. SIMULATOR DESCRIPTION

The infrastructure topology of the railway line has been developed in a graphical manner using the OpenTrack tool (Nash & Huerlimann, 2004), which supports modelling a railway line by means of double vertex graphs (Figure 2-8). This allows defining the infrastructure topology in a graphical manner. Graphic elements have attributes that can be precisely configured by the user. Also, precise data of the rolling stock such as technical characteristics for every Electrical Multiple Unit, including traction efforts and speed diagrams, weight, length, adherence factor and power systems can be introduced. In particular, real data obtained from FGC series 112, 113 and 114 currently in service have been applied.

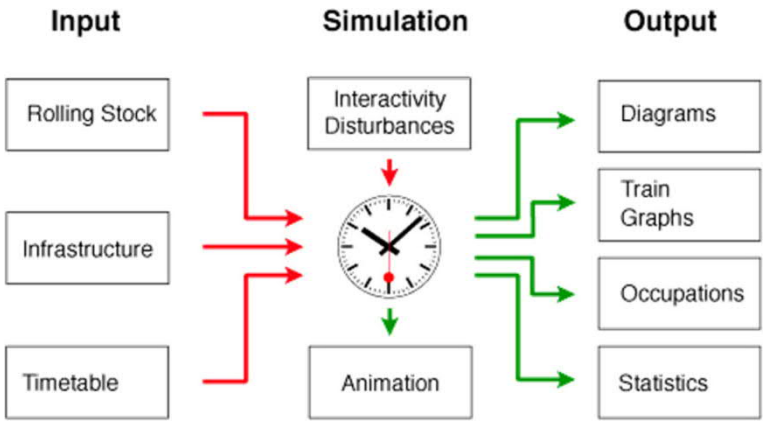

Figure 2-8. Simulator operation process

Signaling and ATP systems have been modeled using real data coming from the actual installation, such as track circuit lengths and gradients, signals, routes between signals, switches and ATP system features.

Additional characteristics of the simulation model are presented in detail in chapter 4.

2.4.2. LINE SECTION DESCRIPTION

The Gràcia-Sarrià section presents some conditions that make it particularly interesting for its analysis. It is an especially congested section, also Sarrià station has been remodeled recently with the aim of improving its capacity, and further improvements to the section are still required to be implemented. Therefore, it turns out to be a good testing ground to analyze its transport capacity possibilities.

2.4.3. DESCRIPTION OF THE TRAFFIC PATTERN

The simulated timetable of the line shows that in the line section from Gràcia to Sarrià, and from 8 to 9 hours during weekdays, 21.8 trains per hour are circulating in direction to Sarrià.
Those trains moving from Gràcia to Sarrià have a particular behavior, which is that half of them do not stop at three of the stations of the interval: Sant Gervasi, La Bonanova and Les Tres Torres. This makes the study of this section key when it comes to determining its Operative Capacity (C_{ope}). Table 2-3 shows the simulated timetable which illustrates the aforementioned characteristics.

Position	Line	Departure	Position	Line	Departure
1st	S1	8:00:00	12th	L6	8:28:30
2nd	L6	8:01:00	13th	S1	8:33:00
3rd	S2	8:05:30	14th	L6	8:34:00
4th	L6	8:06:30	15th	S2	8:38:30
5th	S1	8:11:00	16th	L6	8:39:30
6th	L6	8:12:00	17th	S1	8:44:00
7th	S2	8:16:30	18th	L6	8:45:00
8th	L6	8:17:30	19th	S2	8:49:30
9th	S1	8:22:00	20th	L6	8:50:30
10th	L6	8:23:00	21st	S1	8:55:00
11th	S2	8:27:30	22nd	L6	8:56:00

Table 2-3. Simulated timetable of trains departing from Gràcia with destination Sarrià (08:00-09:00)

The repeating cycle between Gràcia and Sarrià during the described part of the service is hence formed by 2 trains, one stopping at all 7 stations and another one stopping only at 4 of them.

The simulator is used to obtain the compressed time T in seconds of the traffic pattern, simulating the trains up to the limit where their circulations would be affected (UIC, 2004). Table 2-4 shows the main parameters of the compressed pattern simulated and its Time vs Distance diagram can be found in Figure 2-2.

Parameter	Value
Dwell Time at stations	30 s
Compressed Cycle Time (2 trains, Sarrià direction)	289s

Table 2-4. Main parameters of the simulated compressed pattern

Figure 2-9 gives an example of the unhindered speed profile computed in the case study for the routes from Gràcia to Sarrià. This simulated speed profile has been compared with real data from the line and the results show its good accuracy.

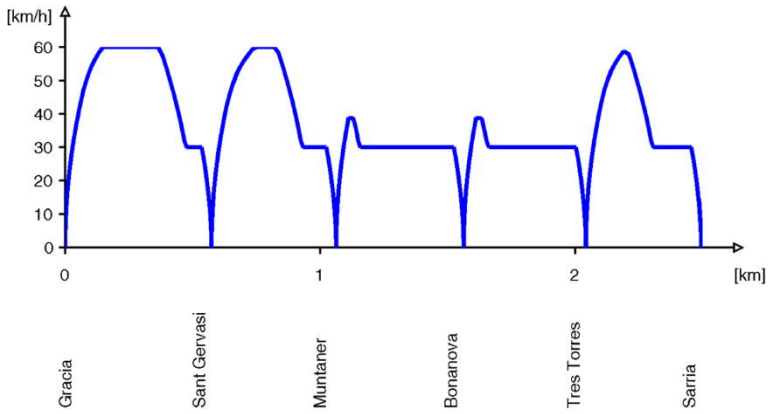

Figure 2-9. Simulated speed profile of a train circulating from Gràcia to Sarrià using the ATP system. Train not hindered by other circulations and stopping at all stations

2.4.4. TRIANGULAR FUZZY DWELL TIMES

To consider uncertainty in dwell times they have been modeled as triangular fuzzy numbers. The membership function is defined as follows, where T_{Dk} is the core of the fuzzy dwell time (equation 2-22, Figure 2-10):

$$\widetilde{\boldsymbol{T}}_{\boldsymbol{Dk}}(\mathbf{x}) = \begin{bmatrix} o & if & x < T_{Dk}{}^{\underline{\alpha}} \\ \frac{x - T_{Dk}{}^{\underline{\alpha}}}{T_{Dk} - T_{Dk}{}^{\underline{\alpha}}} & if & T_{Dk}{}^{\underline{\alpha}} \le x \le T_{Dk} \\ \frac{T_{Dk}{}^{\overline{\alpha}} - x}{T_{Dk}{}^{\overline{\alpha}} - T_{Dk}} & if & T_{Dk} \le x \le T_{Dk}{}^{\overline{\alpha}} \\ 0 & if & x > T_{Dk}{}^{\overline{\alpha}} \end{bmatrix} \quad (2\text{-}22)$$

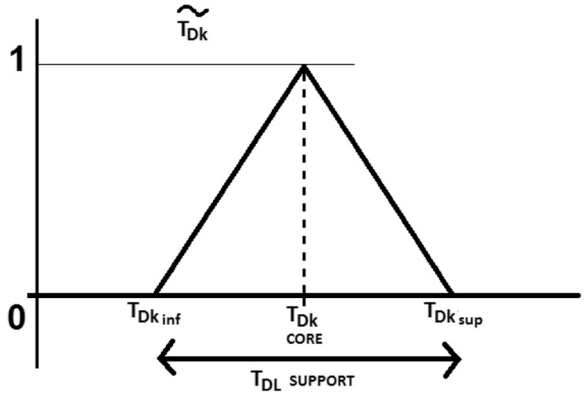

Figure 2-10. Diagram of Fuzzy Dwell Times. Triangular implementation.

To analyze the impact of the core variation, the core T_{Dk} of the dwell time interval used ranges from 20 to 40 seconds at each stop. This range is considered as the most possible considering the operating experience in the section regarding dwell times. Also, the influence of the support variation of the fuzzy distribution (from lower to upper alpha-cut limit) has been tested, making it range from 15 to 25 seconds (equation 2-23, T_{DL} between 15 and 25s).

$$T_{DL} = T_{Dk} + T_{Dk}{}^{\overline{\alpha}} - (T_{Dk} - T_{Dk}{}^{\underline{\alpha}}) = T_{Dk}{}^{\overline{\alpha}} + T_{Dk}{}^{\underline{\alpha}} \quad (2\text{-}23)$$

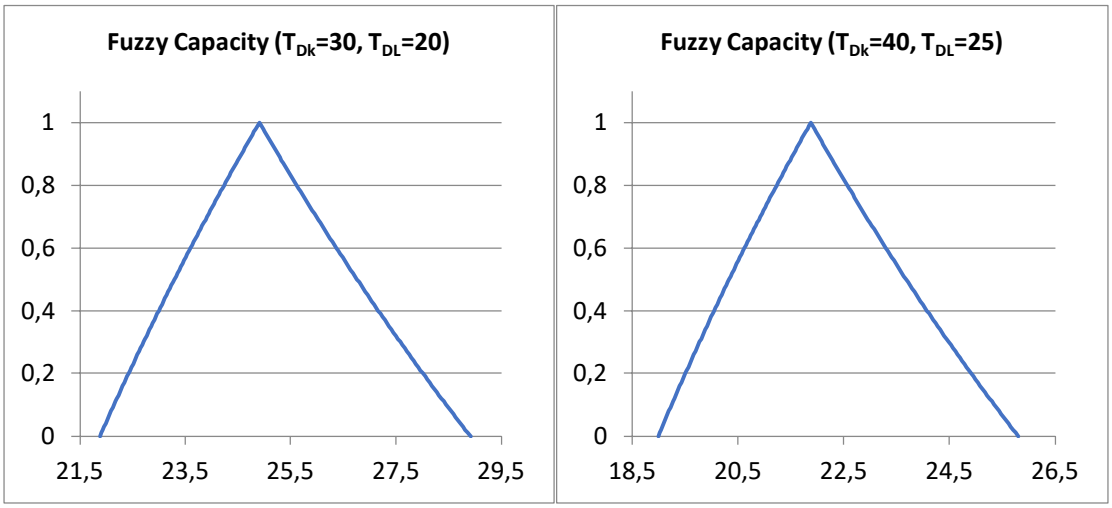

Figure 2-11: Examples of fuzzy capacity obtained using triangular Dwell Times distribution and different values of T_{DL} and T_{Dk}

The three practical applications from the perspective of the traffic operator previously proposed in section 2.2 are analyzed. Also, a sensitivity analysis is presented with the objective of assessing the impact of variations in the core and support of the fuzzy dwell times.

2.4.5. FIRST APPLICATION: IS THE OPERATIVE CAPACITY ACHIEVABLE?

The first step is to verify whether the operative capacity C_{ope}, defined by the operator, is below the Fuzzy Maximum Capacity. According to the simulated timetable, this section of the line is operated with a C_{ope} of 21.8 trains per hour during the rush hour of the daily service. The fuzzy maximum capacity shown in Figure 2-12, has been obtained using a fuzzy dwell time with a T_{Dk} of 30 seconds and a T_{DL} of 25 seconds, which are typical values according to the experience of the operator of the line.

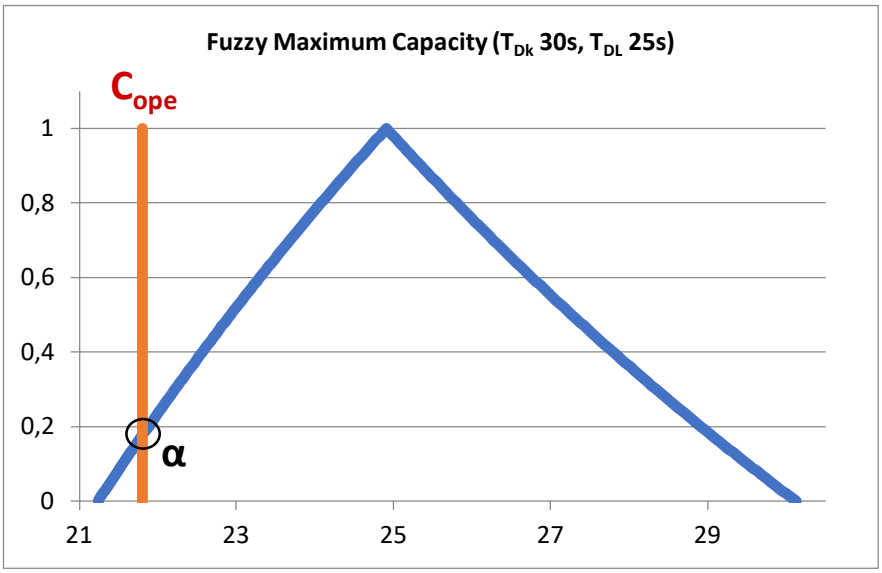

Figure 2-12. Fuzzy Maximum Capacity $\tilde{C}$ (T_{Dk} 30s, T_{DL} 25s)

Under that scenario, the possibility and necessity measures of fulfilling the fuzzy constraint $\tilde{C} \geq C_{ope}$ are calculated as:

$$N\left(\tilde{C} \geq C_{ope}\right) = 1 - \Pi\left(\tilde{C} < C_{ope}\right) = 1 - \alpha \quad (2\text{-}24)$$

$$N\left(\tilde{C} \geq C_{ope}\right) = 1 - \alpha = 0{,}83 \quad (2\text{-}25)$$

$$\Pi\left(\tilde{C} \geq C_{ope}\right) = 1 \quad (2\text{-}26)$$

The results show that, even during the rush hour, the first requirement is accomplished with a high degree of certainty, although no reliability margin has been considered yet to face an incident without disrupting the service.

For the sake of comparison, by using the same input parameters but with crisp values (considering the core of the Fuzzy Dwell times) instead of fuzzy ones, the following maximum capacity is obtained:

$$C = \frac{3600 \cdot n}{T} = \frac{3600 \cdot 2}{289} = 24{,}91 t/h \quad (2\text{-}27)$$

The crisp value shows that the C_{ope} of 21.8 trains per hour would always be accomplished. Hence, taking uncertainty into account by means of fuzzy numbers provides the operator richer and more complete information than just using crisp values.

2.4.6. SECOND APPLICATION: APART FROM BEING ACHIEVABLE, DOES THE OPERATIVE CAPACITY KEEP ENOUGH RELIABILITY MARGINS?

In a similar way to the first application, in the second one the operative capacity is

compared considering the margin proposed by the UIC in terms of the occupancy time rate. This allows considering a buffer to absorb certain delays that may happen during the normal operation of the section. The fuzzy occupancy time rate $\widetilde{U}$ shown in Figure 2-13, is obtained using a fuzzy dwell time with T_{Dk} of 30s and a T_{DL} of 25s.

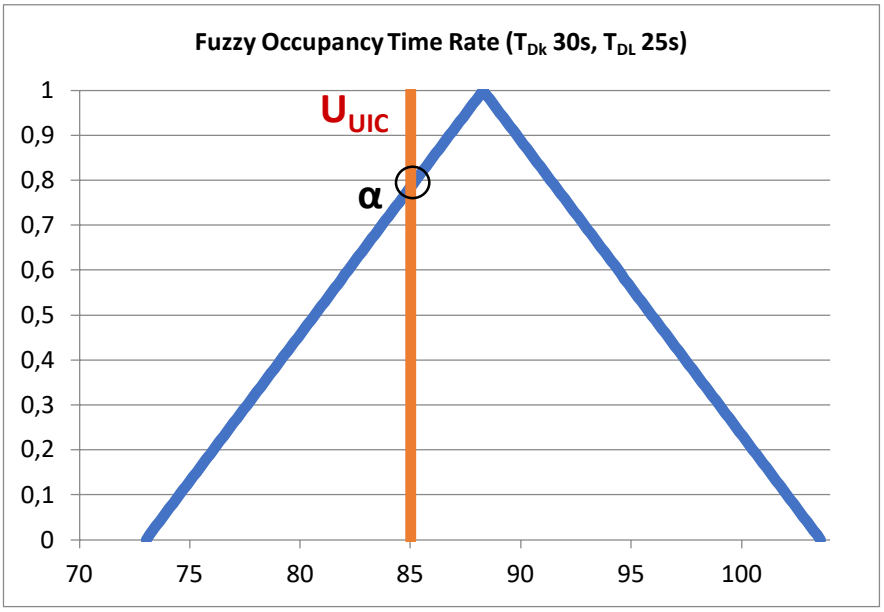

Figure 2-13. Fuzzy Occupancy Time Rate $\widetilde{U}$ (T_{Dk} 30s, T_{DL} 25s)

Given the reference occupancy time rate U_{UIC} of 85% proposed by UIC, the possibility and necessity measures of fulfilling the fuzzy constraint $\widetilde{U} \leq U_{UIC}$ are calculated as:

$$\mathrm{N}\left(\widetilde{U} \leq U_{UIC}\right) = 1 - \Pi\left(\widetilde{U} > U_{UIC}\right) = 1 - 1 = 0 \qquad (2\text{-}28)$$

$$\Pi\left(\widetilde{U} \leq U_{UIC}\right) = \alpha = 0{,}78 \qquad (2\text{-}29)$$

In light of the results, the second requirement can be accomplished with a degree of certainty during the rush hour of operation. If the same calculation is performed using crisp values, the following results are obtained:

$$\frac{C_{\mathrm{ope}}}{C} 100 \leq U_{\mathrm{UIC}} \qquad (2\text{-}30)$$

$$\frac{22\ \mathrm{t/h}}{24{,}91\ \mathrm{t/h}} 100 = 88{,}32\% > 85\% \qquad (2\text{-}31)$$

In this case, the perception about the degree of certainty is lost entirely. Then, as a conclusion, it would seem that the operative capacity is not achievable by any means if the occupancy time rate value of 85% proposed by the UIC is taken into consideration.

2.4.7. THIRD APPLICATION: CALCULATION OF THE HIGHEST C_{OPE} THAT FULFILLS THE RECOMMENDED UIC OCCUPANCY TIME MARGINS WITH A TARGET POSSIBILITY/NECESSITY VALUE

The values of possibility and necessity that fulfill the required UIC occupancy time rate value and C_{ope} of the section at the same time can be found by calculating equation 2-32. The numerical values have been obtained by using a T_{Dk} value of 30s with a T_{DL} of 25s, and α_{obj} = 0,5 and $\mathrm{N}_{\mathrm{obj}}$ =0:

$$\prod\left(\frac{C_{\mathrm{ope}}}{U_{UIC}}100 \leq \tilde{C}\right) = \alpha_{\mathrm{obj}} \quad (2\text{-}32)$$

$$\prod\left(\frac{C_{\mathrm{ope}}}{85\%}100 \leq \tilde{C}\right) = 0{,}5 \quad (2\text{-}33)$$

$$C_{\mathrm{ope}} = 23{,}18\ \mathrm{t/h} \quad (2\text{-}34)$$

Therefore, under the Dwell Times defined and using the uncertainty parameters set previously, the highest C_{ope} that fulfils the target possibility is 23,18 trains per hour.

Another example on this same scenario could be obtained. If the operator imposes a higher level of certainty on the fulfillment of the UIC Occupancy Time margins, he will impose a necessity level instead (that is stricter than a possibility level). In the following example, C_{ope} is calculated by setting N_{obj}=0,42 and α_{obj}=1:

$$\mathrm{N}\left(\frac{C_{\mathrm{ope}}}{85\%}100 \leq \tilde{C}\right) = 0{,}42 \quad (2\text{-}35)$$

$$C_{\mathrm{ope}} = 19{,}75\ \mathrm{t/h} \quad (2\text{-}36)$$

In this case, the calculated C_{ope} is 19,75 t/h. When a necessity level is imposed, the operative capacity calculated is lower than the one obtained when a possibility value is imposed.

2.4.8. SENSITIVITY ANALYSIS

This section is aimed to show a sensitivity analysis of the capacity considering different fuzzy dwell time possibility distributions. To this end, all fuzzy maximum capacities have been obtained for fuzzy dwell times with core T_{Dk} ranging from 20 to 40 seconds and support T_{DL} ranging from 15 to 25 seconds. Figure 2-14 depicts the values of the C_{ope} that comply with possibility α_{obj} = 0,7 (and thus, a necessity value of 0).

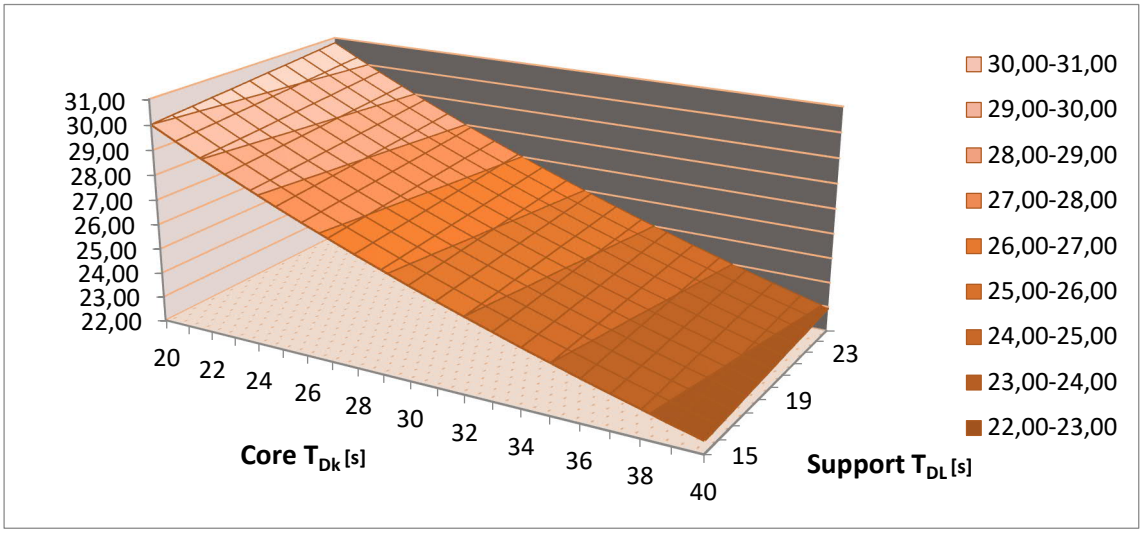

Figure 2-14. Operative Capacity sensitivity analysis. Possibility (α_{obj})=0,7 Necessity=0

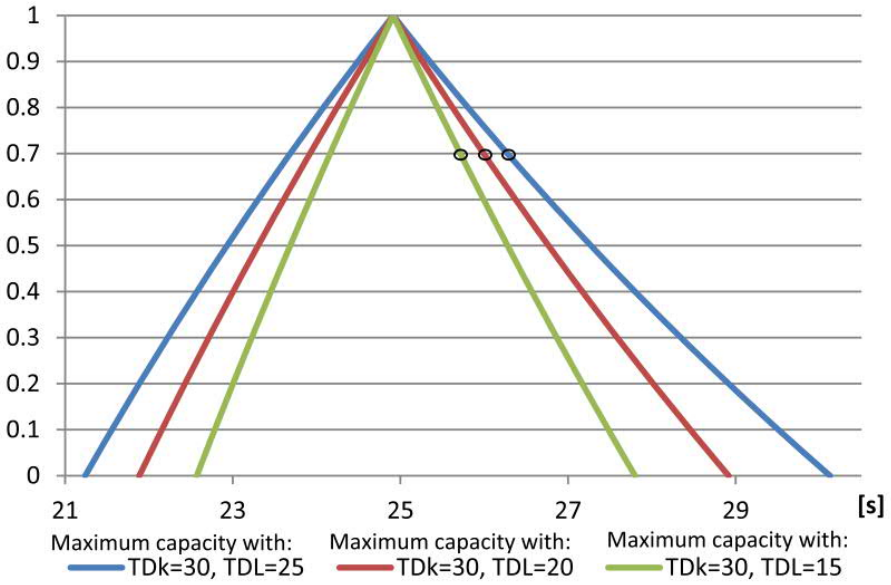

Figure 2-15. Influence of T_{DL} support variation on Fuzzy Maximum Capacity and C_{ope} (Possibility=0.7, Necessity=0)

The operative capacity figure shows that, for any particular value of T_{Dk}, a certain sensitivity in T_{DL} can be observed. As a conclusion, in general the wider the T_{DL} span, the higher the C_{ope} obtained. This happens because when the support of the fuzzy maximum capacity is bigger, the calculated C_{ope} for α=0,7 increases. Figure 2-15 shows this behavior in detail for a fixed value of T_{Dk} (30s). The fuzzy capacity is depicted for three different values of T_{DL}.

That is, when the support of $\tilde{T}_D$ increases, lower values of dwell times are considered possible, and for these lower values of dwell times, higher values of maximum capacity are calculated as possible as well.

On the other hand, if a necessity value is imposed, the higher the T_{DL}, the lower the C_{ope}

calculated (see Figure 2-16). In this case, when the support of $\tilde{T}_D$ increases, higher values of Dwell Times are considered possible, and for these values of Dwell Times, lower values of maximum capacity are calculated as possible. Thus, when the target necessity level is imposed, the calculated C_{ope} is lower as the $\tilde{C}$ support increases.

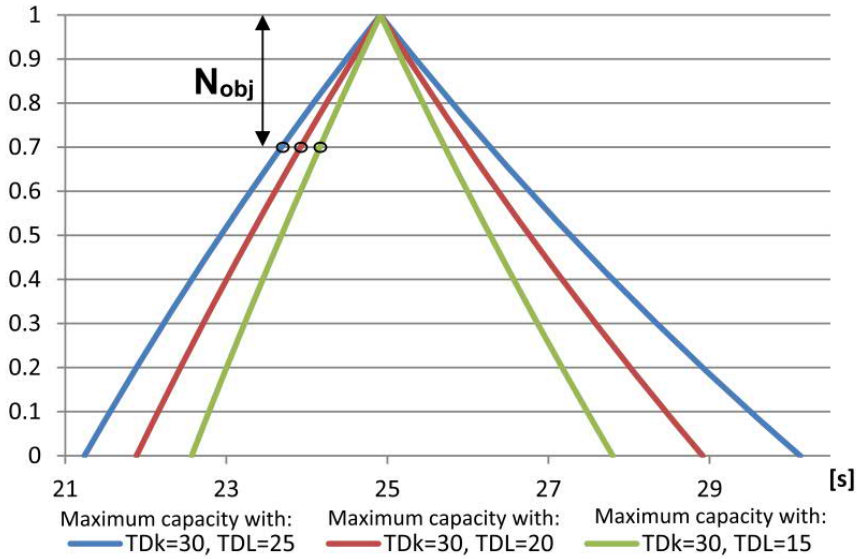

Figure 2-16. Influence of T_{DL} suport variation on Fuzzy Maximum Capacity and C_{ope} (Necessity=0.3, Possibility=1)

Figure 2-17 shows the impact on C_{ope} of modifying T_{Dk} for different values of the necessity value imposed. This time T_{DL} is fixed at 20s. The different curves are obtained by fixing its Necessity value and obtaining the corresponding Operative Capacity values for every T_{Dk} measured.

Then, by making use of this information and his own record of operating experience, the operator can design the timetable in order to maintain an occupancy time rate that allows certain reliability margins.

This procedure could be used to apply the UIC margin recommendations or the operator's own, the later could be specifically defined for the line under operation considering its intrinsic characteristics. This may end up being a better solution than the one-size-fits-all approach of UIC's occupancy time rate guidelines. Also, by adjusting the possibility and necessity target values, the system can be suited to account for a predefined level of uncertainty. The operator expertise again can be the key in its definition.

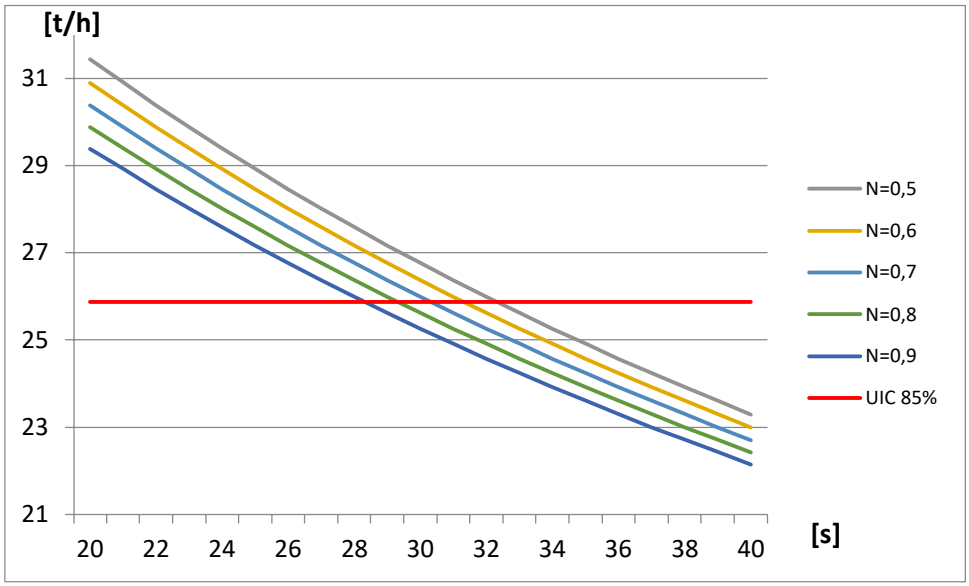

Figure 2-17. Operative Capacity VS T_{Dk} for different values of Necessity. T_{DL}=20s

CHAPTER 3
DESIGN OF INDICATORS TO GUIDE CAPACITY IMPROVEMENTS IN URBAN RAILWAY LINES

3.1. INTRODUCTION: CAPACITY IMPROVEMENTS IN URBAN RAILWAY LINES

The demand for urban transport will increase in 95% until 2050, especially in developing countries where cities are expected to growth hugely in size. Urban dwellers will rise from 4 to 6.4 billion people during the aforementioned period (OECD, 2017).

Railway is one of the most efficient modes of urban public transportation and it has seen an impressive technological improvement during the last few decades. Looking into the future, railway is expected to be a cornerstone to alleviate congestion problems in big cities and metropolis all around the globe.

Specifically, demand for railway urban transport is expected to increase 60% and this rise will put a lot of pressure on current infrastructures. Therefore, city planners and infrastructure managers will have to take complex decisions in order to increase the capacity of current railway networks. Building completely new infrastructures as well as the use of different rolling stock that allow more capacity are options on the table, but they are quite expensive ones. Also, they tend to be constrained by political momentum and funding, the rhythm of which is usually not synchronized with social transportation needs.

But, before engaging in lengthy and costly upgrading processes, there are other easier and convenient options that need to be analyzed. Transport capacity limitations in railway networks are caused to a great extent by high dwell times at stations, especially in high density urban lines. These dwell times at stations can be harmful to capacity availability particularly during the rush hour when a great number of passengers make use of the service.

An extended dwell time for a particular train can disrupt the following one, that will have to reduce its speed or even come to a complete stop. This situation happens because the minimum departure-arrival itinerary times (I_{DAmin}) required between trains following each other are not fulfilled, and then the following train is too close

to the previous one and its movement gets disrupted. So, it becomes key to improve the departure-arrival itinerary times at the station in order to improve the capacity at each of them.

I_{DAmin} represents the minimum interval corresponding to the time passed between the start of the movement of the first train from a station until the stop in the same station of a following train without any disturbance caused to the second train by the signaling system. So that an increase of one more second in the moment of departure of the first train would start causing disruption to the following train.

In the railway environment different types of capacity are typically used (Abril et al., 2008). Firstly, the Theoretical Capacity associated to the passage of trains in trains per hour through a station of a metro line is obtained as:

$$C = \frac{3600}{H_{min}} \quad (3\text{-}1)$$

Where:

$H_{min} = I_{DAmin} + DT$ [s]
H_{min}: Minimum Headway [s]
I_{DAmin}: Minimum interval for 2 trains at a station [s]
DT: Dwell Time [s]

Theoretical Capacity is the maximum value that could be obtained in a line under ideal conditions without any existing delays. Practical Capacity considers some additional buffer times that are introduced in the timetable to absorb possible delays so that a more realistic measure of line capacity is offered. But it is still a fixed value that does not fully account for disruptions and delays since it considers that trains are not disrupted by the signaling system. See section 2.1 for additional detail on the definition of the different types of capacity in the literature.

However, during real line operation in urban lines, traffic can be heterogeneous and service disruptions and delays are often suffered. These disruptions are quite common during the rush hour in urban lines close to saturation, therefore it is necessary to take these situations into account when it comes to system design.

In the aforementioned situation, trains travel in disrupted conditions caused by the signaling system and the measures of Theoretical and Practical Capacity of the line are not useful anymore since these measures are not enough to account for slowdowns caused by the signaling system that control the flow of trains throughout the line. Therefore, it is necessary to define new Capacity Indicators for urban lines that are useful to characterize urban railway installations where it is frequent to have trains travelling in disturbed conditions. The definition of this new Capacity Indicators is the challenge addressed by the present chapter.

Some authors present different methods to evaluate between several transport improvement alternatives, like Nalmpantis et al. (2019) who present an application of a Multi-Criteria Decision Analysis (MCDA) method, the Analytic Hierarchy Process (AHP), that based on expert's evaluation allows deciding among different transport implementations.

Zhang et al. (2020) propose an interesting multi-objective optimization method based on particle swarm optimization to choose among different designs for a railway line, considering both economic and environmental considerations. The method is not applied specifically to urban railway lines, but to optimize railway alignment design decisions.

For its part Luteberget et al. (2019) present a verification technique and tool to be used at the design phase of the installation to assess its capacity; this allows processing different design solutions to choose the optimal one among them. The authors use an approach that avoids using a model including both discrete and continuous elements, therefore losing the precision that these methods bring. Also, their study does not consider the specificities of disturbed urban railway lines, as described in Chapter 1 of this document.

In Haramina & Talan (2018) the feasibility of a timetable and infrastructure improvement in a suburban line to be expanded from single to dual-track line is validated. They perform several iterations in station areas to obtain the desired results and also applied different simulation scenarios to validate their conclusions. The work is based on comparing capacity available of the existing single-track design with the modified dual-track one; the work is not aimed to finding the best possible design solution but to validate the improvements of the new proposal.

In Burdett (2016) is presented an analytical model suitable to identify capacity expansions in railway systems, considering track duplications and subdivisions of sections. The model allows to decide in each case which design approach is more effective and furthermore of application to new railway networks. The authors use Theoretical Capacity and do not consider the effects of disturbances in the line and their consequences in Capacity values.

Lai & Wang (2012) also present a method to evaluate the capacity benefits of implementing new advanced signaling system in a Taiwanese line. The method uses fixed values to model the real installation and does not consider line saturation conditions.

A model to evaluate the impact on a mixed railway network of different expansion proposals is presented in Rosell & Codina (2020). The mathematical programming-based model is mainly focused on increasing freight transportation and they show its application to a regional network located in the Mediterranean Corridor. A Pareto efficiency analysis is applied in order to find the optimal result of investment executed and operating costs obtained out of the model application. The aim of the model is to compare different design possibilities; it is not aimed to find the optimal

solution for every different proposal.

In Ljubaj et al. (2017) the authors present an analysis of the bottlenecks of a line with the aim of increasing its capacity utilization without resorting to expensive new investments. The use of a simulator allows the assessment of different situations and changes in the infrastructure. Ljubaj et al. (2018) displays a similar approach allowing the selection and discard of different line upgrade alternatives according to their justification in terms of capacity increase. In Ljubaj et al. (2019) a double-track line and its planned upgrade to allow for bi-directional traffic are analyzed and simulated in order to assess the economic feasibility of the line upgrade. These three previous works are based on determining if the proposed signaling solutions improve the existing model and its bottlenecks, not on finding the optimal solution for every bottleneck found in the line.

Macroscopic models used to analyze the future capacity of networks using forecast data are presented in Reinhardt et al. (2018). The models can be used to find bottlenecks under different demand scenarios and to choose between a set of possible capacity expansions, helping proper placement of future railway infrastructure investments. The authors present a macroscopic solution to improve freight capacity, the application of it to urban railway lines and their specificities is not shown in the paper.

In Jensen et al. (2017) a model to calculate railway infrastructure occupation and capacity consumption by using a stochastic simulation of delays is presented. It is applied to different scenarios and it does not require a timetable, allowing optimization of the infrastructure by considering different train sequences. The model uses a stochastic simulation solution and compares different signaling alternatives, it is not aimed to find the optimal solution for every bottleneck.

Additionally, several works have been published related to the modelling of disturbed railway systems. In Abril et al. (2008) the authors show a summary of the different methods available to calculate railway capacity, also it shows some simulation methods that allow the reproduction of train interactions and knock-on delays. In Huang et al. (2019) the authors review the disturbances in high-speed lines and considering train interval, disturbance length, occurrence time and disturbance influence, they present a model based on K-Means clustering that allows analyzing disturbances in real-time operation.

A mesoscopic simulation method that allows calculating values of capacity at stations is proposed in Zhong et al. (2018). It also considers the presence of random disturbances although only of train and operation delays.

In Zieger et al. (2018) the authors present a simulation model to analyze the influence of buffer times distributions on capacity and level of service (expected waiting time for trains). The model is also compared to the STRELE framework to assess its validity and differences.

A technical exercise with the aim of analyzing the capacity increments allowed by the installation of a new signaling system, but without modifying the existing layout, is presented in Marcianò et al. (2019). A model of the real installation is created to simulate its behavior under predefined levels of capacity load. The results obtained allow sensing the improvements in terms of capacity that will be obtained by the planned investment but without fully considering the performance of the system under disrupted conditions.

An approach to simulate a single direction suburban railway system based on the Nagel-Schreckenberg model is showcased in Becker & Schreckenberg (2018). This approach uses a cellular automaton with the application of stochastic dwell times; this was previously used to reproduce jamming effects in roads. The implemented solution does not consider the effect of disturbances in the line and their effect on trains through the signaling system.

In Shekhar et al. (2019) the authors demonstrate a railway junction simulator with mixed traffic based on Python. It uses graph theory to simulate the junction and select the best path available to traverse it and identify existing bottlenecks. It also allows comparing the effects of changes in the infrastructure, but also lacks the analysis of the effect caused by disturbed conditions in the line.

The concept of dynamic capacity consumption is introduced in Goverde et al. (2013); random distributions of delays are used to model real-life operations to simulate disturbed conditions. A modular dispatching system based in a microscopic model of the line under test is shown. The model does not focus on finding the optimal solution for the bottlenecks of the line, but on validating the improvements obtained with the implementation of the proposed design solutions.

In Gašparík et al. (2018) a simulator based on RailSys is presented. It allows simulating railway lines with mixed traffic and introducing different delays into the system with the aim of calculating the line capacity value, but without considering the specificities associated with urban railway lines.

In table 3-1 the summary of the different references found in the literature is presented. Also, a specific detail about their focus on disturbed or dynamic conditions is emphasized.

	Dynamic Ind.	Notes	Reference
Choosing between alternatives	✗	AHP based on expert's evaluation	(Nalmpantis et al., 2019)
	✗	Optimization method, particle swarm	(Zhang et al., 2020)
	✗	Design phase, choosing optimal solution	(Luteberget et al., 2019)
	✗	Feasibility of expansion in a suburban line	(Haramina & Talan, 2018)
	✗	Duplications and subdivisions of sections	(Burdett, 2016)
	✗	Benefit of new signaling system in a line	(Lai & Wang, 2012)
	✗	Evaluate different expansion proposals	(Rosell & Codina, 2020)
	✗	Determining if proposed solutions improve the existing model and its bottlenecks	(Ljubaj et al., 2017), (Ljubaj et al., 2018), (Ljubaj et al., 2019)
	✗	Macroscopic models to analyze capacity	(Reinhardt et al., 2018)
	✗	Stochastic sim of buffer times	(Jensen et al., 2017)
	Disturbed	**Notes**	**Reference**
Modelling of systems	✓	Reproduction of train interactions & knock-on delays	(Abril et al., 2008)
	✓	K-Means clustering, disturb. real-time operation	(Huang et al., 2019)
	✓	Mesoscopic, values of capacity at stations	(Zhong et al., 2018)
	✓	Influence buffer times on capacity & level of service	(Zieger et al., 2018)
	✗	Analysis capacity increments, new signaling system	(Marcianò et al., 2019)
	✗	Cellular automaton, stochastic dwell times	(Becker & Schreckenberg, 2018)
	✗	Graph theory to simulate junction	(Shekhar et al., 2019)
	✓	Random delay distributions, real operations	(Goverde et al., 2013)
	✓	Mixed traffic delays: calculating line capacity	(Gašparík et al., 2018)

Table 3-1. State of the art – Summary table

In this work, indicators designed to guide capacity improvements in urban lines with high occupancy stations are presented. Their specific goal is the removal or impact reduction of bottlenecks in stations that reduce the overall capacity of the line. Also, the presence of service disruptions due to hindered circulations during the rush hour and their effects has been considered in the indicators design.

These novel indicators ease the decision-making process required when it comes to making investments on the infrastructure to guide capacity enhancements. When different scenarios are presented to the infrastructure manager, having the proper tools to choose among them results in a long-term very valuable asset.

The following parts of the chapter are organized as follows. A Model to calculate disturbed capacity indicators using a rail simulator and real data coming from the actual installation is presented in section 3.2. The case study is shown in section 3.3.

The proposed installation design improvements and the results obtained are shown in section 3.4.

3.2. DISTURBED CAPACITY MODEL

3.2.1. MODEL DESCRIPTION

In this section, a model to calculate disturbed capacity indicators using a rail simulator and real data coming from the actual installation is proposed. This model allows considering disturbances in nodes and the process of choosing between different signaling solutions.

This model uses as a measurement of disturbance between two consecutive trains, considering the time of departure of two trains from two consecutive nodes (A and B):

$$T_{\mathrm{BT}} = T_{\mathrm{BTP}} - (T_{\mathrm{D2B}} - T_{\mathrm{D1A}}) \qquad (3\text{-}2)$$

Where:

T_{D2B} = Time of departure of 2nd train from station B
T_{D1A} = Time of departure of 1st train from station A
T_{BT} = Difference between departure times between two consecutive trains from two consecutive stations
T_{BTP} = Limit of difference between departure times of two consecutive trains from two consecutive stations; times lower than this value imply a disturbance to the movement of the second train

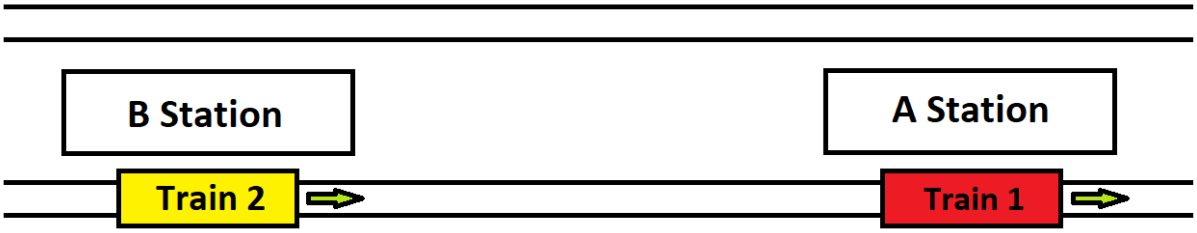

Figure 3-1. Disturbance measurement for two consecutive trains

During nominal performance, trains depart from the station B and arrive to station A without being disturbed through the signaling system by any previous train, with T_{D2B}-T_{D1A}>T_{BTP}. As T_{D2B}-T_{D1A} gets reduced, the following train of the pair starts to be disturbed by the previous one (T_{D2B}-T_{D1A})<T_{BTP} and T_{BT}>0. This situation is presented when for example Train 1 increases its dwell time at the station B. Therefore, the T_{BT} value when positive shows that two trains are running beyond their limit of disturbance and its value denotes for how many seconds that limit is being surpassed. So, it is a measurement of disturbance between two consecutive trains.

Figure 3-2 shows the running time between the departure of a train from Station B and its arrival to Station A as a function of the increase in Dwell Times beyond the

point when the movement of the second train gets disturbed by the first one in Station A. For values of T_{BT} smaller than 0, the time of movement of the second train is constant since the movement of the train is not hindered by the signaling system because there is enough distance between both trains to run without disturbing each other.

From $T_{BT} > 0$ the movement of the second train is affected by the signaling system, increasing therefore its time of movement. In $T_{BT} = 0$ the Theoretical Capacity value can be found, that is the Capacity value that allows trains to move as close as possible without affecting each other. In this point, the difference between the departure of the first train from A Station and the arrival of the second one to the same station is I_{DAmin}, which offers the minimum headway without disturbance.

Note that when the T_{BT} value reaches a certain value the train suffers a complete standstill due to the action of the signaling system (Figure 2-2, t of 32s). After this value, the graph of running time is a straight line with an angle of 45º, because for every extra second of T_{BT} the train is stopped one more second due to the action of the signaling system that stops it for one additional second. This increases for one second its running time to the next station.

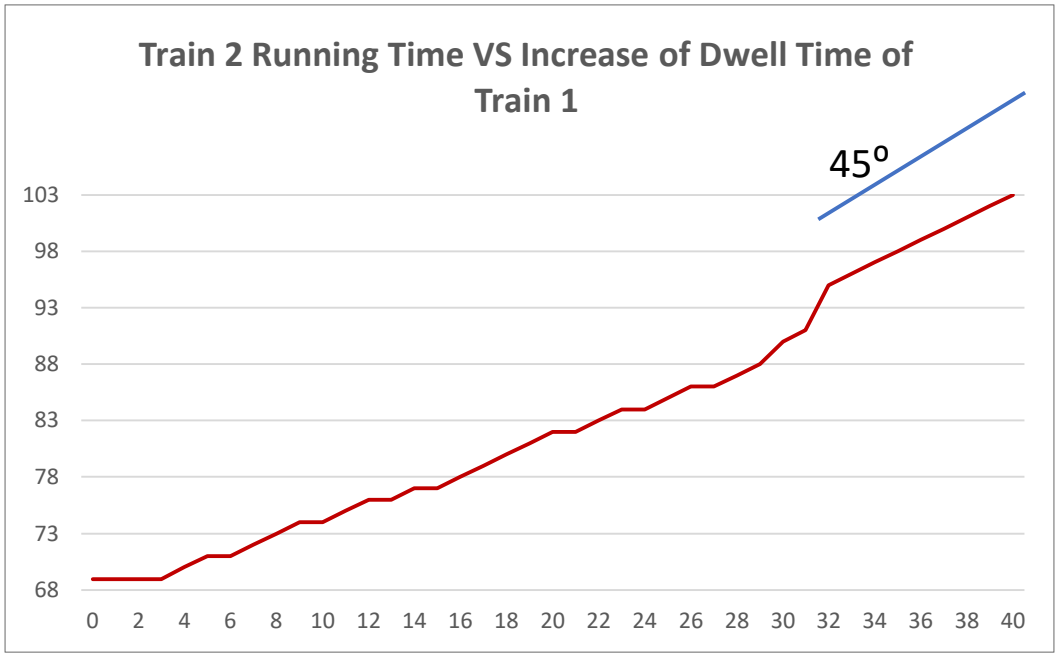

Figure 3-2. Train 2 Running Time (y-axis) versus Increase of Dwell Time of Train 1 (x-axis) after the T_{BTP} limit values

For values of T_{BT} higher than 0 the values of Theoretical Capacity are not useful anymore because the trains are moving in disturbed conditions. In these situations, where T_{BT} is higher than 0, the new indicator of Disturbed Capacity is defined as:

$$C_{\mathrm{D}} = \frac{3600}{H_{\mathrm{D}}} \qquad (3\text{-}3)$$

Where:

$H_D = I_{DAP} + DT$

H_D: Average Disturbed Headway

I_{DAP}: Average Disturbed Interval

DT: Dwell Time

I_{DAP} is the average value of the disturbed departure-arrival interval, it can be calculated as the expected value of the statistical distribution of I_{DA} for values of T_{BT} >0. This distribution is produced during the real service of the line during the period of time under analysis (for example, during the rush hour). H_D is the average disturbed headway value between trains that are moving under disturbed conditions and C_D is the disturbed Capacity value associated to the installation under those disrupted circumstances.

The expected I_{DAP} value is obtained using:

$$I_{\mathrm{DAP}} = \sum_0^{INF} I_{\mathrm{DA}}(T_{\mathrm{BT}}) \times f(T_{\mathrm{BT}}) d(T_{\mathrm{BT}}) \qquad (3\text{-}4)$$

Where $f(T_{BT})$ represents the statistical frequency of the disturbances (variable T_{BT} for $T_{BT} > 0$) experienced during the time period of the real line service under analysis. $I_{DA}(T_{BT})$ is the interval between departure and arrival of two consecutive trains to a station produced for every value of T_{BT}.

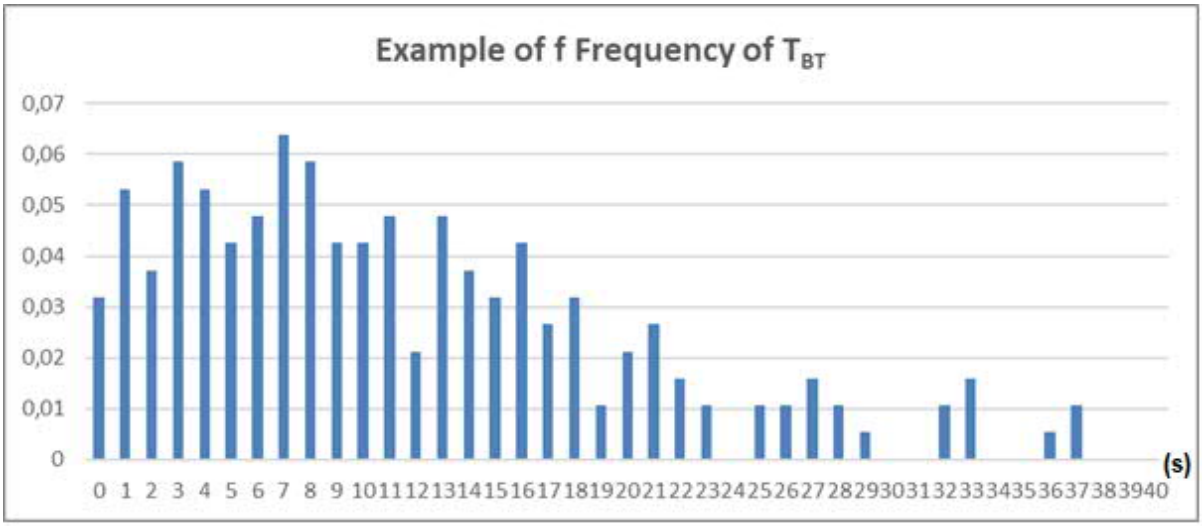

Figure 3-3. Example of normalized statistical frequency of $T_{BT} > 0$ accumulated values (y-axis) versus Increase of Dwell Time of Train 1 (x-axis) after the T_{BTP} limit value

$f(T_{BT})$ is also obtained using statistical analysis of real data during the time zone under study to consider the level of disturbance of the trains approaching the station. This level of disturbance in the station under analysis depends also on the level of disturbances in the previous stations of the line that may generate a ripple effect down the line.

$I_{DA}(T_{BT})$ depends only on the signaling system and the train speed profile and for an existing installation, that can be obtained using statistical analysis of train movements real data. In the cases of greenfield or resignaling projects, simulation tools can be used to calculate and evaluate Capacity indicators under disturbed conditions. In Figure 2-9 an example of $I_{DA}(T_{BT})$ is presented, the straight part of the graph corresponds to values of dwell time of train 1 that actually cause train 2 to come to a complete stop.

The second indicator of the line under disturbed conditions is the loss of commercial speed caused by the speed reduction generated in the signaling system. The indicator related to the Disturbed Running Time (T_{RD}) is obtained as the expected value of running times T_R when movements are disturbed, T_{BT} is higher than 0 and the frequency of real disturbance of trains f is known.

$$T_{\mathrm{RD}} = \sum_0^{INF} T_{\mathrm{R}}(T_{\mathrm{BT}}) \times f(T_{\mathrm{BT}}) d(T_{\mathrm{BT}}) \qquad (3\text{-}5)$$

$T_R(T_{BT})$ depends on the signaling system, the train speed profile and on the frequency of disturbed trains arriving to the station. For an existing installation, it can be obtained using statistical analysis of real data of train movements. In the cases of greenfield or resignaling projects, simulation tools can be used to calculate and evaluate it.

In conclusion, two indicators associated to periods involving disturbed trains moving between two nodes have been presented: C_D and T_{RD}. The first one is a measurement of disturbed capacity, while the second measures the loss of service quality produce under these situations. Both indicators need to be considered to design and redesign signaling systems; a reasonable compromise must be achieved.

3.2.2. MODEL STEPS

In this section the procedure to apply the proposed model is presented. The model requires the following steps to perform the complete evaluation:

1. The minimum $(T_{D2B} - T_{D1A})$ value (T_{BTP}) that allows unhindered operation and the associated I_{DAP} value are both obtained with the use of the simulator. To accomplish this several 2-train simulations are performed with the goal of launching the second train as close as possible to the first one, without its movement being disturbed by the signaling system due to the proximity to the first train.

2. Using the simulator to perform several runs and starting from the T_{BTP} value, the T_{BT} value is increased from 0 in successive simulation steps with the aim of obtaining the $I_{DA}(T_{BT})$ characteristic curve of the node under study. In this step, the movement of the second train is always affected by the first one. Then, the I_{DA} curve obtained with all the iterations simulated represents a curve of how the second train is

affected by the signaling system as it gets closer to the first one. In the same way, the running times of the second train $T_R(T_{BT})$ are obtained following the aforementioned iterative simulation process.

3. Furthermore, with the analysis of real installation data coming from the operator the frequency of real disturbances is calculated. That is the frequency of the T_{BT} variable. From this data and using the minimum T_{BTP} value that allows unhindered operation found in step 1, the numbers are filtered to obtain the frequency of $T_{BT} > 0$ values that cause the disturbance in the installation during real operating conditions.

4. The average I_{DAP} value is the basis of the indicator of disturbed capacity. This average value is obtained as a result of the weighted average of all I_{DA} values obtained with the simulator weighted by their real occurrence frequency in the node under study for $T_{BT} > 0$. The indicator meaning is clear: it is the average interval considering the real statistical disturbance level existing in the node and it offers information regarding the true level of disturbance experienced in the node. Also, the C_D value is calculated and gives information of the disturbed Capacity Value associated to the installation.

5. The indicator of average disturbed running time T_{RD} is obtained in a similar way to the indicator of disturbed capacity. It is obtained as the average of all disturbed route times (for $T_{BT} > 0$) weighted by their frequency of their occurrence.

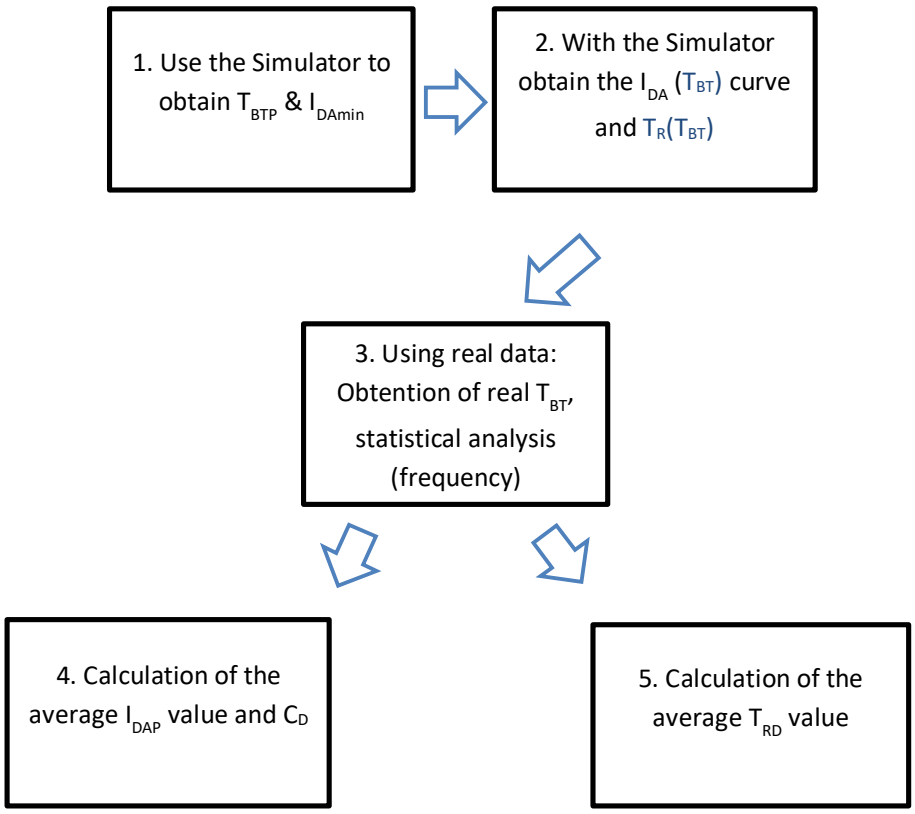

Figure 3-4. Model Flow Chart

Both indicators of Disturbed Capacity and Average Disturbed running Time T_{RD} constitute a useful tool to decide among different signaling alternatives to redesign existing signaling installations.

Regarding Disturbed Capacity C_D it gives precise information about the installation usage under disturbed conditions. This indicator is more useful than the Theoretical Capacity one because it considers the interactions between trains; therefore, considering the resulting effects they produce to each other and that are transferred through the signaling system.

The different signaling design alternatives are simulated and then the aforementioned indicators are obtained. The best signaling solution will be the one offering better indicators. This implies a higher level of capacity in real conditions that include disturbed circulations, but at the same time keeping in check the average route time.

3.3. CASE STUDY

In this section an example of resolution of the model presented in the previous section is described.

3.3.1. LINE DESCRIPTION

The FGC Barcelona-Vallès line has been chosen to apply the methods described in the previous sections. FGC (Ferrocarrils de la Generalitat de Catalunya) is a railway company which operates several lines in Catalonia, a region located at the northeast of Spain. And the Barcelona-Vallès line connects Barcelona with the cities of Terrassa and Sabadell, going through the Collserola range.

Figure 3-5. Map of FGC Barcelona-Vallès line

The Barcelona-Vallès infrastructure is fitted with an ATP (Automatic Train Protection) safety system which is in charge of supervising the train speed and applying the penalty brake in the event of safety conditions not being fulfilled. This line is equipped with continuous data transmission through coded track circuits with a speed codes implementation scaled to 90/60/45/30/0 km per hour. It enforces speed limits and movement authorities ensuring safety of train movements by comparing the current train speed to the permitted speed limit. Speed is limited by the system to protect routes of other trains in the installation or due to other existing constraints in the line.

With the aim of obtaining precise times of the itineraries in the installation, a parametric model of the section has been implemented using a simulation tool. This tool allows modelling line profile data and track topology as well as rolling stock and the routes for each interlocking of the line.

The station of Provença is arguably one of the most congested nodes in the whole network. It is a key station serving several lines: L6, L7, S1, S2, S5, S6 and S7. Hence, it constitutes a perfect testing ground to apply the tools shown in previous sections.

3.3.2. SIMULATOR DESCRIPTION

The infrastructure topology of the railway line has been developed in a graphical manner using the OpenTrack tool (Nash & Huerlimann, 2004), which supports modelling a railway line by means of double vertex graphs (Fig. 7). Graphic elements have attributes that can be precisely configured by the user. Also, precise data of the rolling stock such as technical characteristics for every Electrical Multiple Unit, including traction efforts and speed diagrams, weight, length, adherence factor and power systems can be introduced. In particular, real data obtained from FGC series 112, 113 and 114 currently in service have been applied.

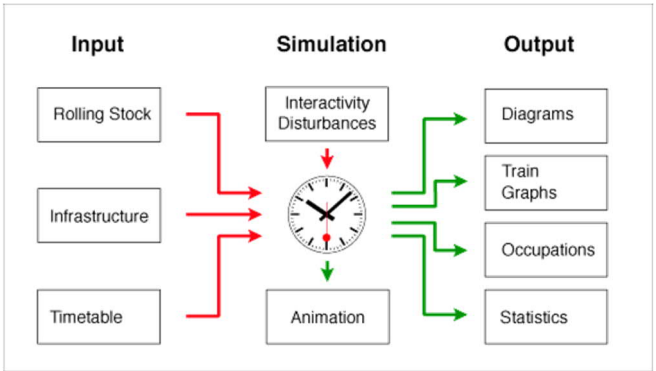

Figure 3-6. Simulator operation process

Signaling and ATP systems have been modeled using real data coming from the actual, such as track circuit lengths and gradients, signals, routes between signals, switches and ATP system features.

Additional characteristics of the simulation model are presented in detail in chapter 4.

3.3.3. NODE DESCRIPTION

The current Provença station was opened in 1929 and has nowadays a passenger density of 4700 passengers per hour during the rush hour, that value only surpassed by Plaça Catalunya in the Barcelona-Vallès line. This density is expected to be increased even more during the next years and the station has been remodeled in 2019 to keep up with this upcoming passenger increment.

3.3.3.1 DESCRIPTION OF THE TRAFFIC PATTERN UNDER ANALYSIS

The traffic pattern under analysis is formed by the movement of trains between Gràcia and Provença stations towards Plaça Catalunya. Therefore, trains leave Gràcia station alternatively from platforms 2 (GR8) and 4 (GR10).

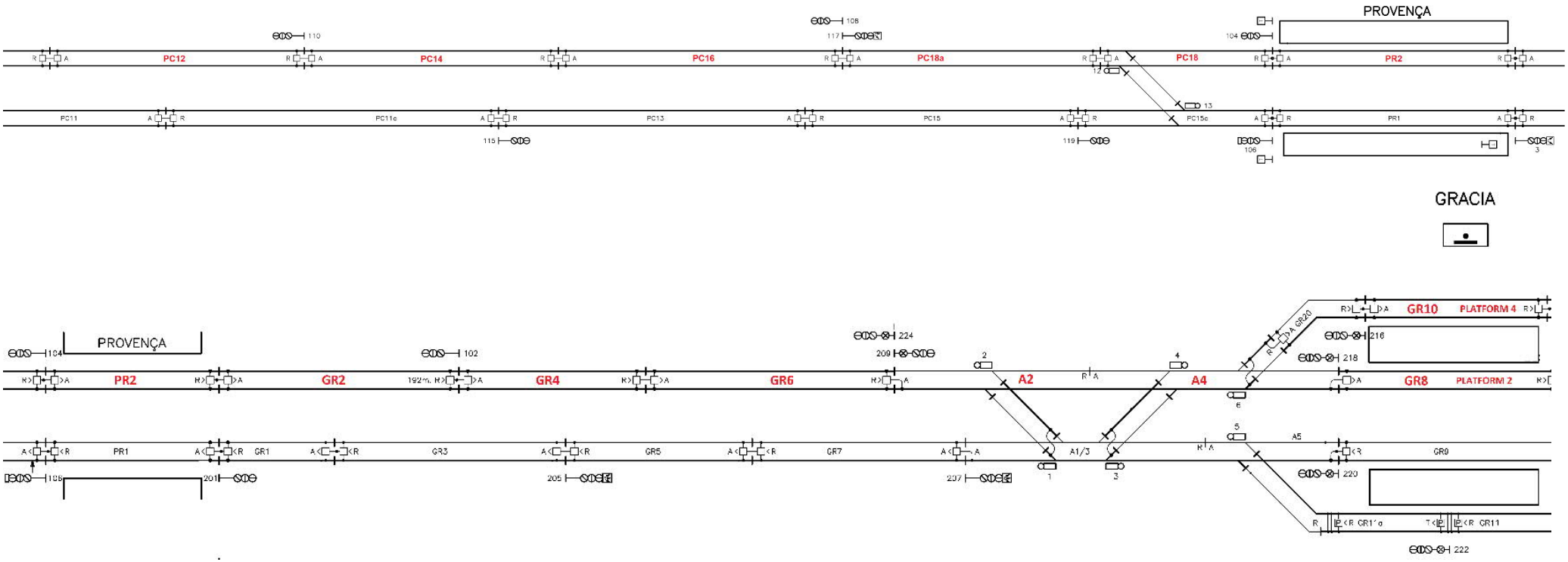

Figure 3-7. Track layout in Gràcia – Provença section

The movement of trains follows a route through track circuits A4, A2, GR6, GR4, GR2 and PR2 which corresponds to the platform in Provença station. The ATP system implementation follows the design shown in Table 3-2.

Right: Train in Track Circuit **Down:** Occupied Track Circuit	A2	GR6	GR4	GR2	PR2	PC18	PC18a	PC16	PC14	PC12
-	60/60	60/60	60/60	60/60	60/60	60/60	60/60	60/60	60/60	60/60
PC12	60/60	60/60	60/60	60/60	60/60	60/30	60/30	30/0	0	-
PC14	60/60	60/60	60/60	60/60	**60/30**	30/30	30/0	0/0	-	
PC16	60/60	60/60	60/60	**60/30**	30/30	30/0	0/0	-		
PC18a	60/60	60/60	60/60	**60/30**	30/0	0/0	-			
PC18	60/60	60/60	**60/30**	30/0	0/0	-				
PR2	60/60	**60/30**	30/0	0/0	-					

Table 3-2. ATP Speed values allowed in section Gràcia – Provença

The codes follow the definition XX/YY, where XX is the maximum speed in the current track circuit while YY is the permitted track speed allowed at the end of the current track circuit.

The codes received by the second train through the continuous data transmission through the coded track circuits are shown on the table 3-2. They depend on the track circuits occupied by the previous train, the closer the trains are the more restrictive the speed limits received by the following train become. This is because the signaling system protects the second train route from colliding with the previous route, which means that the following train reduces its commercial speed due to the presence of the previous train and the reduced speed codes it generates after it.

3.3.4. APPLICATION OF THE MODEL STEPS TO THE CASE STUDY

In this section the application of the Model Steps to the Case Study is presented:

Steps 1&2. Obtention of the minimum T_{BTP} (limit of disturbances), I_{DAmin}, $I_{DA}(T_{BT})$ and $T_R(T_{BT})$

In this step the T_{BT} of the first train is increased sequentially by increasing the Dwell Time of the first train using the simulator, the results are shown in Table 3-3.

$$T_{\mathrm{BT}} = T_{\mathrm{BTP}} - (T_{\mathrm{D2B}} - T_{\mathrm{D1A}}) \quad (3\text{-}6)$$

Level of disturbance in Provença T_{BT}	Departure-Arrival Interval I_{DA}	Train 2 Running Time	$-(T_{D2B} - T_{D1A})$	Train position in disturbance T1 / T2
-7	69	69	0	-
-6	68	69	1	-
-5	67	69	2	-
-4	66	69	3	-
-3	65	69	4	-
-2	64	69	5	-
-1	63	69	6	-
0	62	69	7	-
1	61	69	8	PC18 / GR4
2	60	69	9	PC18 / GR4
3	59	69	10	PC18 / GR4
4	59	70	11	PC18 / GR4
5	59	71	12	PR2 / GR6
6	58	71	13	PR2 / GR6
7	58	72	14	PR2 / GR6
8	58	73	15	PR2 / GR6
9	58	74	16	PR2 / GR6
10	57	74	17	PR2 / GR6
11	57	75	18	PR2 / GR6
12	57	76	19	PR2 / GR6
13	56	76	20	PR2 / GR6
14	56	77	21	PR2 / GR6
15	55	77	22	PR2 / GR6
16	55	78	23	PR2 / GR6
17	55	79	24	PR2 / GR6
18	55	80	25	PR2 / GR6
19	55	81	26	PR2 / GR6
20	55	82	27	PR2 / GR6
21	54	82	28	PR2 / GR6
22	54	83	29	PR2 / GR6
23	54	84	30	PR2 / GR6
24	53	84	31	PR2 / GR6
25	53	85	32	PR2 / GR6
26	53	86	33	PR2 / GR6
27	52	86	34	PR2 / GR6
28	52	87	35	PR2 / GR6

29	52	88	36	PR2 / GR6
30	53	90	37	PR2 / GR6
31	53	91	38	PR2 / GR6
32	54	95	39	PR2 / GR6
33	56	96	40	PR2 / GR6
34	56	97	41	PR2 / GR6
35	56	98	42	PR2 / GR6
36	56	99	43	PR2 / GR6
37	56	100	44	PR2 / GR6
38	56	101	45	PR2 / GR6
39	56	102	46	PR2 / GR6
40	56	103	47	PR2 / GR6

Table 3-3. Result values obtained with the simulator (s)

The first column shows the disturbance level reached by the two trains arriving to Provença platform (T_{BT}). The second column shows the interval between the departure of the first train and arrival of the second one (I_{DA}). And the third one is showing the running time of the second train; this time displays directly the affectation produced on the second train by the delay of the first one and its transmission to the second through the signaling system. And the fifth column shows the track circuits where both trains are located when the disturbance is produced.

The 0 value in the first column shows the moment when the second train is receiving the affectation produced by the first one (time resolution in seconds). This means that it is receiving reduced speed codes through the signaling system and these codes are in turn affecting its normal movement.

With this information, the following characteristic curves of the Provença station are obtained.

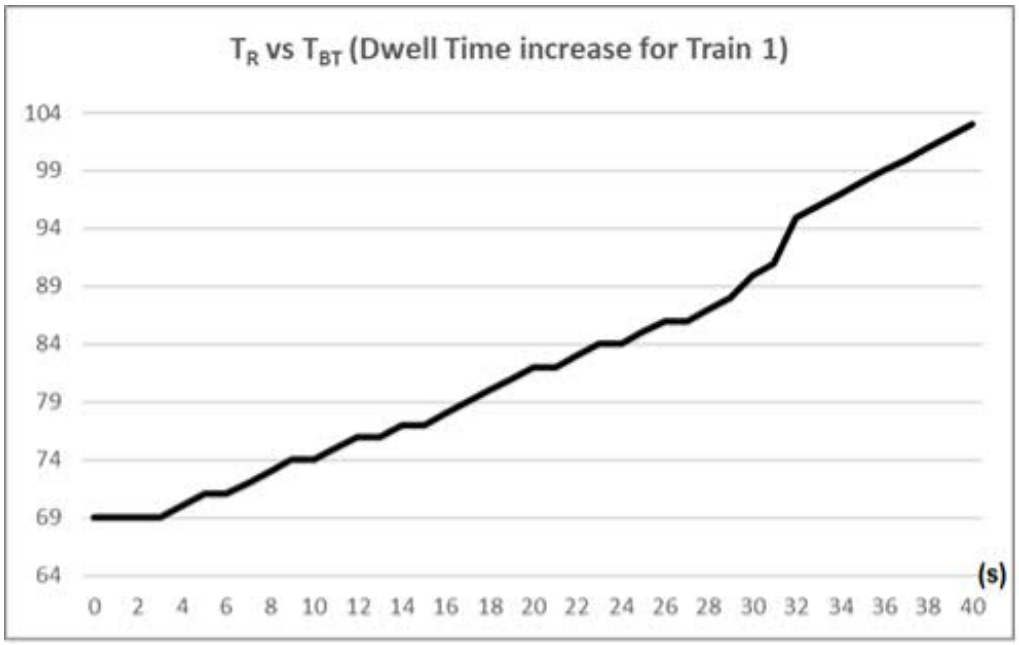

Figure 3-8. TR(TBT) (y-axis) versus T_{BT} (Dwell Time increase for Train 1) (x-axis)

The Figure 3-8 shows the T_R values that correspond to each T_{BT} value; they increase as the level of disturbance between the trains grows. When the following train is stopped completely before continuing its movement (33s in Figure 3-8), the slope shown presents a 45º shape, as explained previously for Figure 3-2.

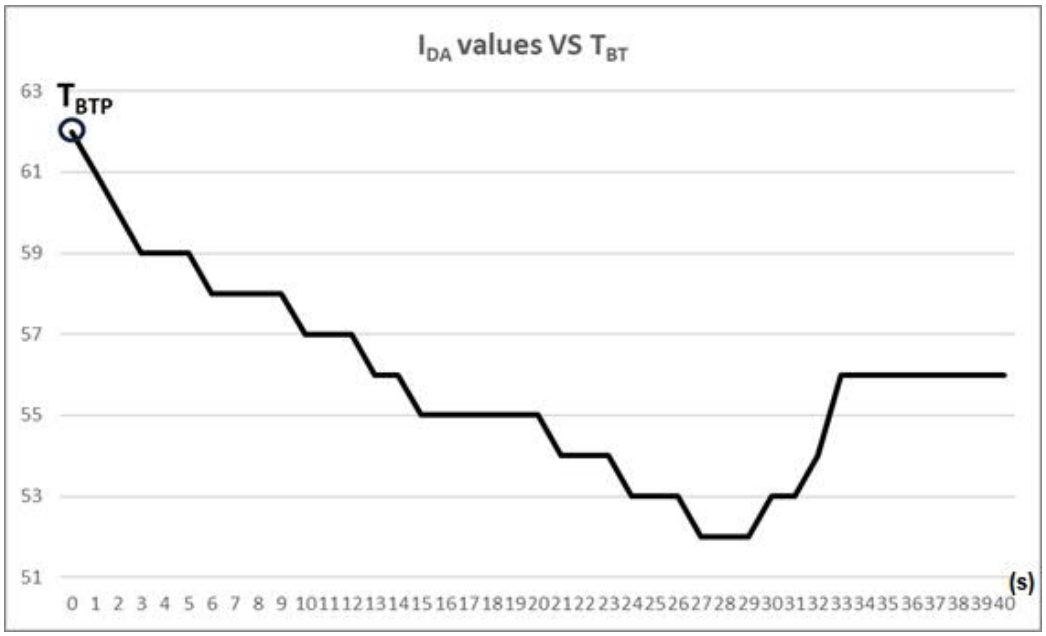

Figure 3-9. IDA values (y-axis) versus for TBT>0

Figure 3-9 shows the I_{DA} value that corresponds to each T_{BT} value. The Dwell Time of the first train arriving to the station is increased sequentially. As the second train gets closer to the first one with each dwell time value increase, the interval between the departure of both trains from their respective stations gets smaller. This means that trains manage to move closer although the second one is

already affected by the signaling system and receives reduced speed codes.

The results show that for an increase in Dwell Time of 28s the I_{DA} value reaches the minimum value of 52s. After that, additional Dwell Time increments also increase the I_{DA} value until the point when the second train is fully stopped by the signaling system during its movement. Therefore, after a T_{BT} value of 33s the I_{DA} value is constant and equals to 56s.

Step 3. Using real data: Obtention of real T_{BT}, statistical analysis (frequency)

Real data coming from the installation have been used for this purpose. The aforementioned data has been obtained from a MoviolaW system, which is a computer-based data logging and replay tool in charge of keeping updated faults and events data continuously coming in real-time from the interlocking. The FGC Barcelona-Vallès line is equipped with Siemens WESTRACE and relay interlockings, models Mk1 and Mk2, the electronic interlockings are all equipped with MoviolaW systems.

The data used in this work was obtained from the MoviolaW systems on October 15th, 2018. They were obtained in database format and have been processed using a tool created specifically for this purpose that allows filtering to acquire only the desired data from the raw file. Figure 3-10 shows an example of the aspect of the data obtained directly from the MoviolaW system prior to its filtering by means of the custom filtering tool.

ID	ID_MNE	VALUE	WT_DATE
46433	14780	0	4:52:47
46434	14463	0	4:52:47
46435	15346	0	4:52:47
46436	15351	0	4:52:47
46437	13560	0	4:52:49
46438	5366	1	4:52:49
46439	8030	1	4:52:49
46440	12953	0	4:52:49
46441	2615	0	4:52:56
46442	2864	0	4:52:49
46443	2864	0	4:52:49
46444	2864	0	4:52:49
46445	2864	0	4:52:49
46446	2746	1	4:52:56
46447	1123	1	4:52:56
46448	8	0	4:52:50
46449	2399	1	4:52:58
46450	8	0	4:52:50
46451	13659	1	4:52:52

Figure 3-10. Raw data coming from Siemens MoviolaW system

Figure 3-10 shows the mnemonics and their changes in value for every second of logged operation time. The values of the field ID_MNE are each one associated to a particular variable of the system, e.g. the status of a specific track circuit has an associated mnemonic whose value can be 0 it the track circuit is occupied or 1 if it is clear. This same principle applies to other elements of the system like points, signals or axle counters. By means of the filtering of these data we can analyze and determine all the changes that took place in the system during a certain period of time.

In this case, the data needed for the calculation is the status of track circuits and the ATP speed codes being injected through the coded track circuits. These codes enforce speed limits and movement authorities to allow the safety of train movements in the installation.

The indicator related to the Disturbed Running Time (T_{RD}), which is also used to calculate the I_{DAP}, is obtained as the expected value of running times $T_R(T_{BT})$ when movements are disturbed (T_{BT} is higher than 0, therefore the second train movement is disturbed), and the frequency of real disturbance of trains f is known. The statistical frequency of T_{BT} can be found in Figure 3-11.

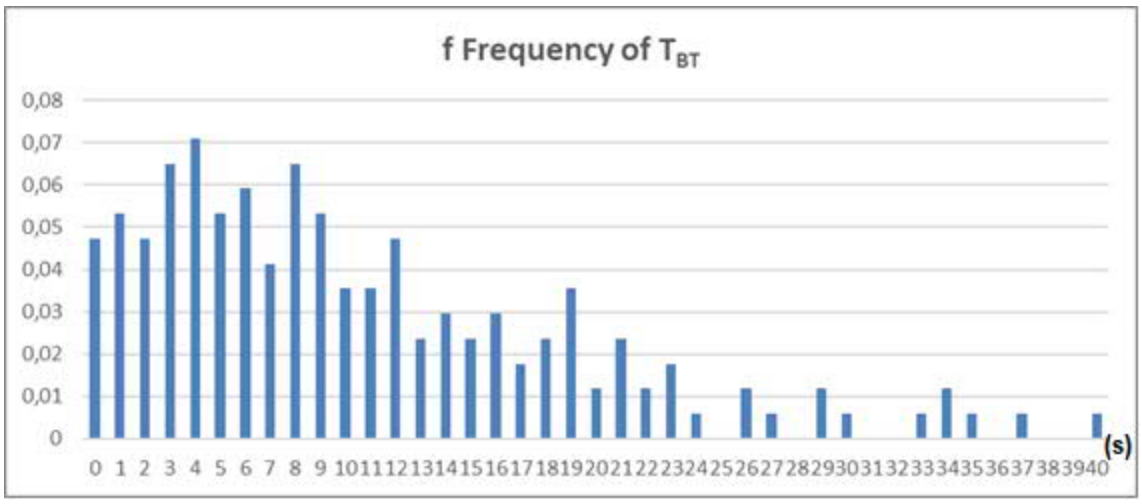

Figure 3-11. Normalized statistical frequency of $T_{BT} > 0$ accumulated values (y-axis) versus Increase of Dwell Time of Train 1 (x-axis) after the T_{BTP} limit value

Step 4. Indicator of disturbed capacity: Average I_{DAP} value

Using figure 3-9 which shows I_{DA} values for T_{BT} value higher than 0 and the statistical frequency of T_{BT}, the average I_{DAP} value is obtained. The I_{DAP} value equals to 57,47s. The average I_{DAP} value indicator is obtained as a result of the weighted average of all I_{DA} values by their real occurrence frequency.

$$I_{\mathrm{DAP}} = \sum_0^{INF} I_{\mathrm{DA}}(T_{\mathrm{BT}}) \times f(T_{\mathrm{BT}}) d(T_{\mathrm{BT}}) \qquad (3\text{-}7)$$

The C_D value is calculated as follows:

$$C_{\mathrm{D}} = \frac{3600}{H_{\mathrm{D}}} \quad (3\text{-}8)$$

$$H_{\mathrm{D}} = I_{\mathrm{DAP}} + DT \quad (3\text{-}9)$$

$$C_{\mathrm{D}} = \frac{3600}{57{,}47+30} = 41{,}16 \text{ Trains/Hour} \quad (3\text{-}10)$$

The minimum interval between trains without any disturbance is 62s. On the other hand, the I_{DAP} value for disturbed trains equals to 57,47s. This value under disturbed conditions is lower; trains move slower but also closer between each other.

Step 5. Indicator of disturbed Route Time: Average T_{RD} value

The average T_{RD} value indicator is obtained as a result of the weighted average T_{RD} values by their real occurrence frequency. It is calculated using:

$$T_{\mathrm{RD}} = \sum_0^{INF} T_{\mathrm{R}}(T_{BT}) \times f(T_{\mathrm{BT}}) d(T_{\mathrm{BT}}) \quad (3\text{-}11)$$

The minimum T_{RD} between trains without any disturbance is 69s. When train movements are disturbed, T_{RD} value equals to 75,07s. These values show the reduction in commercial speed caused by the disturbances to train movements. These disturbances show up in reduced speed codes received by the trains running too close to each other.

3.4. DESIGN IMPROVEMENTS

To obtain the results of the application to the case study, the track layout information and the data in Table 3-4 obtained from the brake distance table are used as inputs.

	92 km/h	62 km/h	46 km/h	31 km/h	21 km/h
-25‰	572.6m	303.3m	195.4m	116.7m	76.4m
0‰	457.7m	243.6m	157.7m	95.2m	63.2m

Table 3-4. Braking distances required to stop the train by levels of track declivity. Values include the level of additional safety applied by the operator.

Declivity value in the section to be redesigned is -25‰. This value is necessary to calculate the distance required to stop the train from every speed value until complete stop. The distance necessary depends heavily on the declivity values, hence they have to be considered to plan the design improvements.

Option A: Modification of track speed codes without any other additional change

Shunted Track Circuit & Lenght	GR6 171.6m	GR4 158.4m	GR2 192m	PR2 120.2m	PC18 109m	PC18a 87m
Case a: PC18	60/60	60/30	30/0	0/0		
Case b: PR2	60/30	30/0	0/0			

Table 3-5. Original ATP Design: Shunting PC18 & PR2

Modifying the track speed codes is the ideal solution as it is relatively the cheapest to be implemented. It only requires an interlocking software update without any change to other track or lineside systems. To check its feasibility, the proper design of the ATP design has to be revised.

Case a: In this case, it has to be checked if a 60/0 reduction could fit in GR2 where we have now a 30/0 reduction. According to table 3-4, that is not possible as it is required a braking distance of 303,3m which is longer than the length of PR2 (120.2m).

Case b: In this case, it has to be checked if a 60/0 reduction could fit in GR4 where we have now a 30/0 reduction. According to table 3-4, that is not possible as it is required a braking distance of 303,3m which is longer than the length of GR2 (192m).

Therefore, a solution only modifying the ATP speed codes design is not feasible,

so this redesign option is in this particular case discarded.

Option B: Change in the interlocking software and redesign the length of track circuits GR2, GR4 and GR6.

To redesign this section, we need to consider the distance required by the train to brake from every speed value until complete stop. Those values are shown in table 3-4. Taking them into account, the adjustment of the length of the track circuits to improve the efficiency of the speed codes applied should be tried.

Technical Discussion: In this case, in case of an emergency brake at the end of GR2 when there is a 30/0 code (previous train in PC18), the train requires 116,7m to brake completely. The reduction 60/0 requires 303.3m, which is a value lower than the combined distance of GR2 and PR2. The following table shows the actual distances presents in the track layout:

Shunted Track Circuit & Lenght	GR6 171.6m	GR4 158.4m	GR2 192m	PR2 120.2m	PC18 109m	PC18a 87m
Train shunting PC18	60/60	60/30	30/0	0/0		

Table 3-6. Original ATP Design: Shunting PC18

Redesign alternatives: There could be several different redesign alternatives to be applied in this situation.

Alternative B1: In order to optimize the braking distances design; GR2 could be reduced to 186,6m (303.3m-116.7m).

Shunted Track Circuit & Lenght	GR6 171.6m	GR4 ~~158.4m~~ 167,3m	GR2 ~~192m~~ 186.6m	PR2 ~~120.2m~~ 116.7m	PC18 109m	PC18a 87m
Train shunting PC18	60/60	60/30	30/0	0/0		

Table 3-7. Modified track circuit distances: Shunting PC18

So according to these calculations, a better design of this section would be to approach the frontiers between track circuits PR2 and GR2 towards the Provença platform by a distance of 3.5m and also between track circuits GR2 and GR4 by a distance of 8.9m. The later modification will also imply moving the signal 102 accordingly.

Alternative B2: In this case, a train applying emergency brake at the end of GR4 and entering GR2 at 30km/h would require 116.7m to stop completely, which is a

distance shorter than the 186.6m currently present in GR2. But this reduction is not feasible if we want to keep the reduction defined in alternative B1; which is reducing from 60/0 in GR2+PR2.

Also, a train applying emergency brake at the end of GR6 and entering GR4 at 60km/h would require 303.3m to stop completely, which is a distance shorter than the 345m currently present in GR4+GR2. Therefore, GR4 could be optimized by making the length of GR2+GR4 equal to 303.3m.

Shunted Track Circuit & Lenght	GR6 ~~171.6m~~ 222m	GR4 ~~158.4m~~ 116.7m	GR2 ~~192m~~ 186.6m	PR2 ~~120.2m~~ 116.7m	PC18 109m	PC18a 87m
Case a2: PR2	60/30	30/0	0/0			

Table 3-8. Modified track circuit distances: Shunting PR2

So according to these calculations the frontier between GR4 and GR6 should be moved towards Provença platform by a distance of 50.6m. This in turn would increase the length of track circuit GR6 up to 222m.

Selection between alternatives: Both alternatives displayed would allow trains to run closer in this section under disturbed conditions. Alternative B2 implies some additional works to modify track circuit limits, therefore it needs to be evaluated it these additional investment makes sense from the operation point of view.

After these modifications, the characteristic curves obtained are the following:

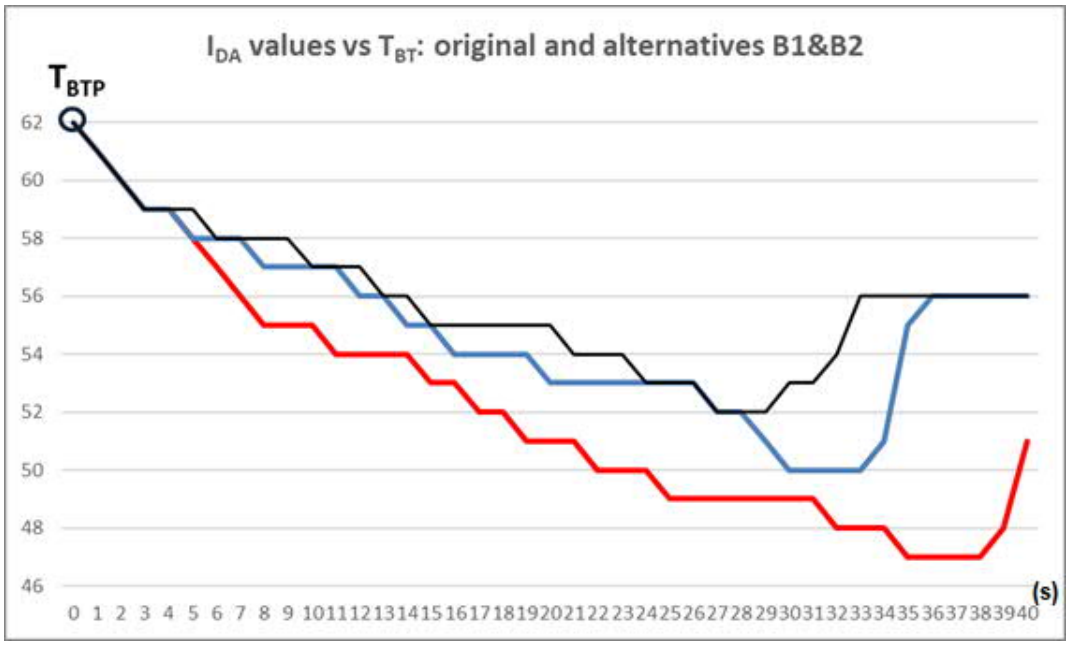

Figure 3-12. I_{DA} values (y-axis) versus for T_{BT}>0, original (black), alternatives B1 (blue) and B2 (red)

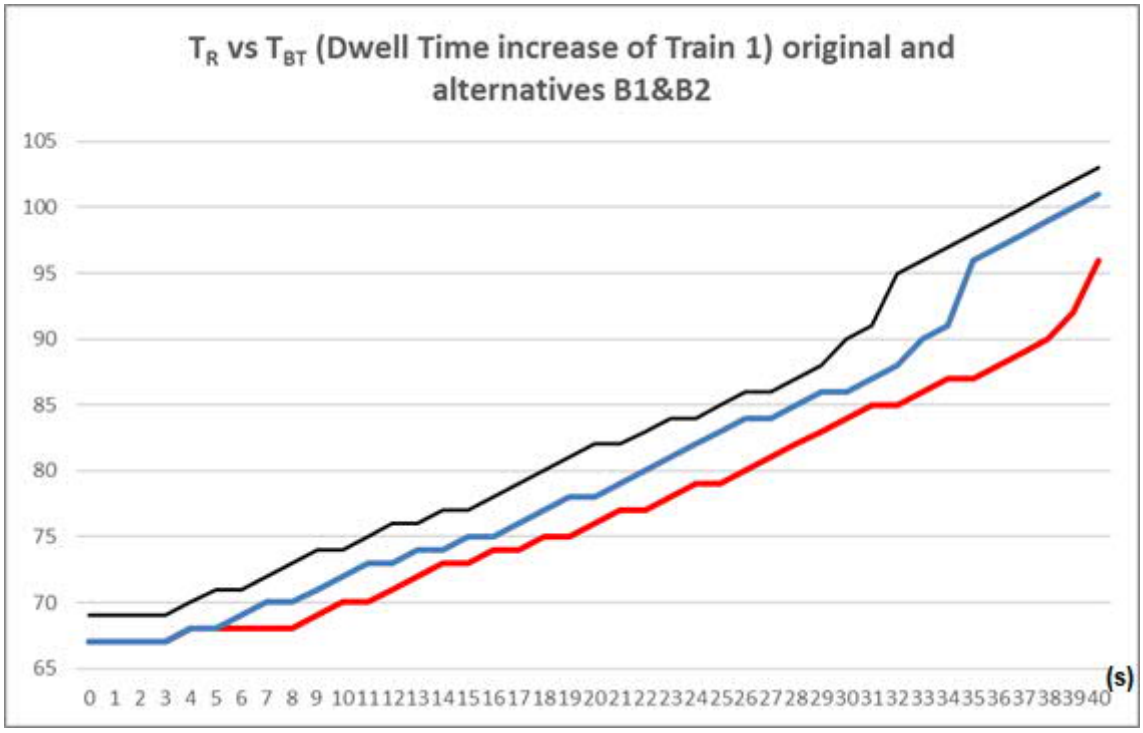

Figure 3-13. $T_R(T_{BT})$ (y-axis) versus Dwell Time increase for Train 1 (x-axis), original (black), alternatives B1 (blue) and B2 (red)

The C_D value is calculated as follows:

$$C_{\mathrm{D}} = \frac{3600}{H_{\mathrm{D}}} \tag{3-12}$$

$$H_{\mathrm{D}} = I_{\mathrm{DAP}} + DT \tag{3-13}$$

$$C_{\mathrm{DB1}} = \frac{3600}{56{,}91+30} = 41{,}42 \tag{3-14}$$

$$C_{\mathrm{DB2}} = \frac{3600}{55{,}47+30} = 42{,}12 \tag{3-15}$$

The following table shows the comparison of values between the base and redesign alternatives B1 and B2:

Indicator	Original	Alternative B1	Alternative B2
I_{DAmin} [s]	52	50	47
I_{Dap} [s]	57,47	56,91	55,47
T_{RD} [s]	75,07	72,56	71,07
C_D [t/h]	41,16	41,42	42,12

Table 3-9. Comparison of indicators between the original and redesigned cases

Both alternatives proposed improve the performance parameters of the original design. Specifically, B2 reduces I_{DAmin} in 9,61%, I_{DAp} in 3,48%, T_{RD} in 5,33% and C_D improves in 2,33%. These performance figures are superior to the ones obtained

by alternative B1, but they require a further modification in the track layout, which is the displacement of the frontier between track circuits GR4 and GR6. This displacement implies the rail welding in the present position of the isolating joints to move them to their new position in the track where their installation will take place. Also, all cabling related to the track circuit connection to the rails needs to be displaced to its new position.

Therefore, alternative B2 is a solution more expensive than B1, although it provides better performance. These indicators allow deciding which is the most interesting solution to be implemented in terms of its cost-efficiency and added value to the performance of the installation. In some cases, little indicator improvements require a high cost of implementation and hence may not be recommended because that money could be better spent in another point of the installation where its impact on system performance is going to be much higher. In many cases, even small percent improvements are beneficial when the line is highly saturated during the rush hour.

CHAPTER 4

SIMULATION MODEL

4.1. OVERVIEW

This work uses a simulation system capable of reproducing accurately the complete behavior of an urban railway installation like the FGC Barcelona-Vallès Line. The system models the behavior of the Rolling Stock operating in the railway line under the constraints defined in the design of the infrastructure and given a timetable and their operations definition. For all the parts combined to make up the model, real data obtained from FGC installations, infrastructure and rolling stock have been used.

In this chapter, a presentation of the different parts of the infrastructure modelled to create the simulation system are presented. Therefore, in this chapter the infrastructure model and the process followed to model its different parts are shown. Also, the model of the signaling system is presented, making a specific mention to the ATP/ATO model that has been implemented into the simulation system. Likewise, the rolling stock model and its calculation process are shown, together with the train movement model and its associated modelling. Lastly, the operations model and the process to create it are also introduced.

The simulation system is created by means of OpenTrack (Nash & Huerlimann, 2004), that is a well-established railway software that allows modelling, simulating and analyzing different types of rail systems. Specifically, for this project it has been used to create the simulation model of the complete FGC Barcelona-Vallès line and to analyze the capacity in stations and also perform running time calculations of train movements.

Therefore, the simulation system allows the user to define input data to create the rolling stock, infrastructure design, timetables definitions and train movements. Then, simulation of operations is carried out using that input data design that has been previously generated.

The particularity of this tool is that it uses a mixed approach between discrete and continuous simulation implementation, as train movements are simulated by means of differential motion equations which are solved continuously. In turn, other elements of the installation present discrete states like, for example, track circuits, signals or predefined delays.

Both train speed and distance travelled are obtained by solving the differential motion equation by means of the Euler's Method, which gives accurate estimated values. And the real occupation state of track circuits and signal aspects also have an affectation on the movement of trains in the installation. Figure 4-1 shows an example of a speed-distance diagram of a train moving from stations A to C and stopping in the middle at station B.

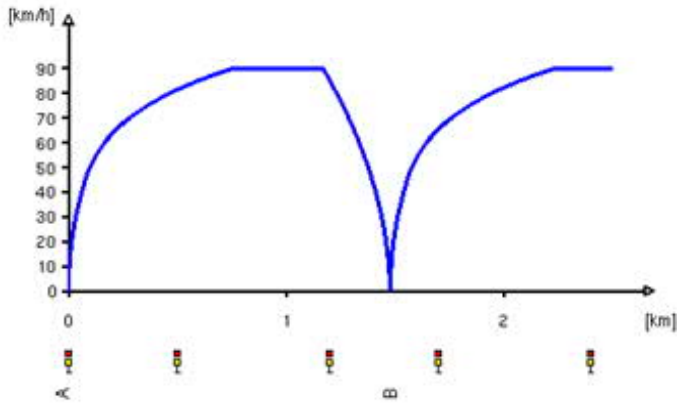

Figure 4-1. Example of a speed-distance diagram

4.2. INFRASTRUCTURE MODEL

The infrastructure model designed uses track circuits, signals and points as basic building blocks to create the installation. The track layout is designed by using data coming from the actual installation currently in service in the line. Figure 4-2 shows an example of Les Planes station. Data obtained from the track layout of the real installation has been used to create its modelized version by using the same distances, gradients and elements placement.

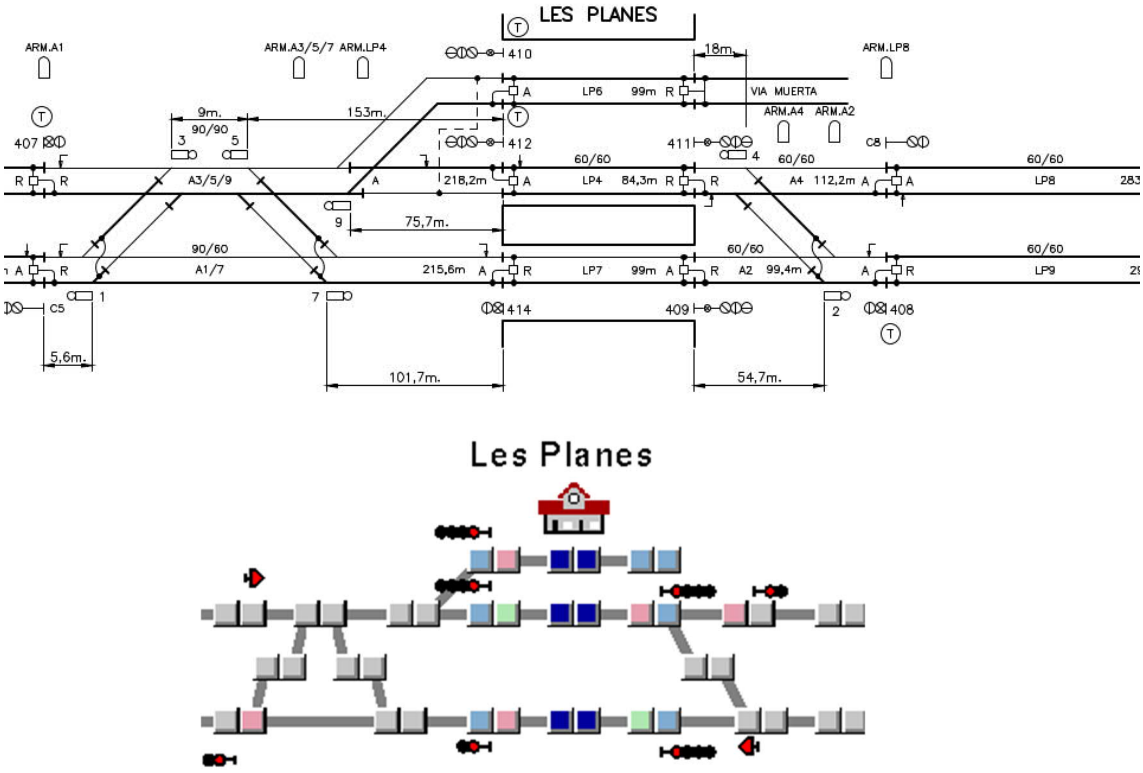

Figure 4-2. Example of a station model: Les Planes. Up: Real Track Layout. Down: Model implementation.

As Figure 4-2 shows, the model is generated by placing elements such as signals and points and connecting them by using track segments. The figure also shows the use of double vertex graphs; every vertex is defined by two joined boxes allowing the definition of different conditions at both sides of the vertex. For example, signals are placed in one of the sides and that is what defines the direction of the movements that the signals are controlling in both movement directions.

The track segments are called edges and are defined with their real properties like their length, gradient, radius and maximum available speed. An example of the design of a track circuit is presented in Figure 4-3.

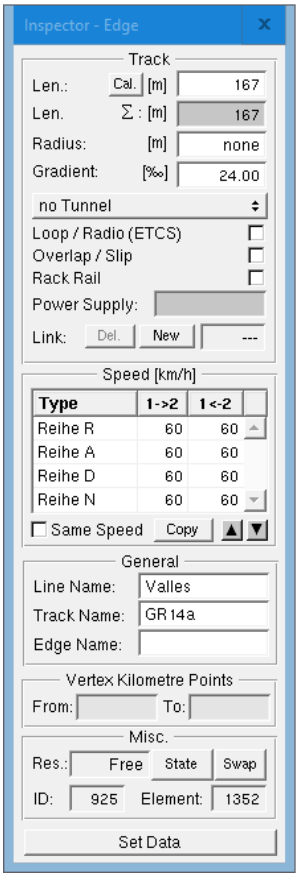

Figure 4-3. Track circuit design example: GR14A

4.2.1. SIGNALING MODEL

The simulator models the signaling system present in the installation and its real behavior. Therefore, each track section can only be reserved by one train at most and every moving train is allowed to stop in the section or sections that are reserved specifically for them. This means that the trains are allowed to move as long as the distance between them is appropriate and their speed permits them to stop under the necessary safety conditions; also, the speed limits required by the track design and current conditions must never be surpassed under any circumstance.

Railway interlockings are the systems present in every line in charge of controlling the safe movement of trains; their behavior is also modelled by the simulator. Two real examples of this kind of systems are shown in Figure 4-4. For trains to perform movements in the line they require a Movement Authority; it gives permission to a train to move from one point of the infrastructure to another one. This means that routes and all the elements that form the route are reserved for the specific train that requires that route, otherwise those elements and the route they form are free. So, in order to successfully reserve a route, it is required that all the elements that form the route are available for it and not blocked by any other route or condition present in the system.

Figure 4-4. Left: Electrical Relay Interlocking. Right: Electronic Interlocking

For the train to complete a route it requires that another route or at least a part of it is free at the end of the reserved route or after its Limit of Movement Authority; this is called a Route Overlap. Overlaps are necessary to ensure safety conditions for the train, even if it is stopping at the end of the route (i.e. a train stopping at a station platform requires an additional free track length after the end of its route to ensure that enough safety distance to allow it to stop safely is available. This additional distance could be required in case of a brake failure or any other kind of system fault. This requirement mandatorily applies in an ATP application design like the one currently present in the FGC Barcelona-Vallès line.

In Distance to Go systems, which is a different kind of ATP application, this requirement is not always necessary. In DTG mode, the train has a map of the line implemented in the On-Board system, and also receives its current position in the line through APR passive transponders located throughout the entire length of the line.

4.2.2. ATP / ATO MODEL

The Barcelona-Vallès line is equipped with an ATP system that supervises the speed of the trains to make sure safety conditions are always fulfilled. The line is equipped with a speed codes implementation scaled to 90/60/45/30/0 kilometers per hour. The 45 code is only available in some parts of the line with an ATP implementation based on Frequency Modulated technology.

The simulated model allows the setting of different track speed limits in every track circuit depending of the status of the signals; this allows designing into the simulator the real behavior of the ATP design present in the Interlocking systems of the line. To do so, in the simulator all signals are equipped with signal aspects and the possible speeds available at their position are defined. Also, the routes associated to each signal are configured in the same way.

Figure 4-5 shows an example of an ATP codes sequence. The Movement Authority shown allows Train B to move until it arrives to the track circuit with a 30/0 code. A free circuit with a 0/0 code needs to be reserved as a safety buffer in this type of signaling systems. During the movement, Train B will have to adapt its movement speed to the maximum speed actually allowed by the signaling system (90 / 60 / 30). In its last authorized circuit, Train B will have to stop until Train A frees its current track circuit, thus allowing Train B to move beyond its current Limit of Movement Authority. When Train A frees its current track circuit, the speed codes present between both trains will change allowing train B to move beyond its current Limit of Movement Authority which will have been moved forward.

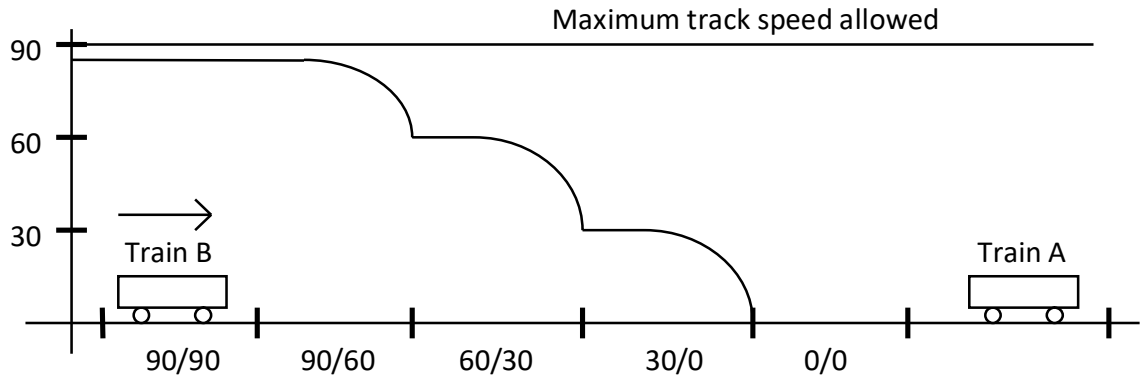

Figure 4-5. Track reservation and ATP codes applied

4.3. ROLLING STOCK MODEL

FGC uses two different train compositions in the Barcelona-Vallès line, units UT113 and UT114. Real data coming from the installation has been used to model the rolling stock of this project. The models use technical specifications of the trains such as tractive effort/speed diagrams (Figure 4-7), weight of the wagons and locomotives, their length, maximum speed, resistance factor and rotating mass factor among other parameters.

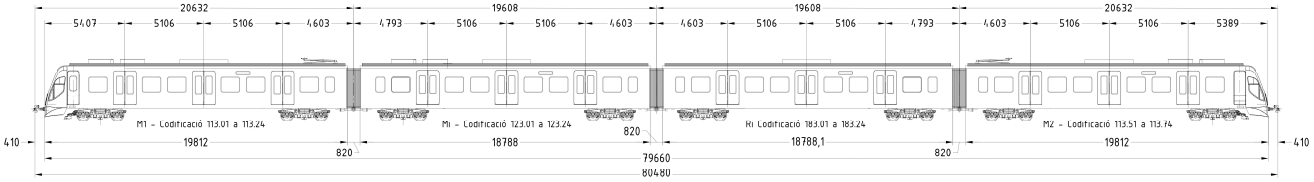

Figure 4-6. Train Unit UT113 FGC

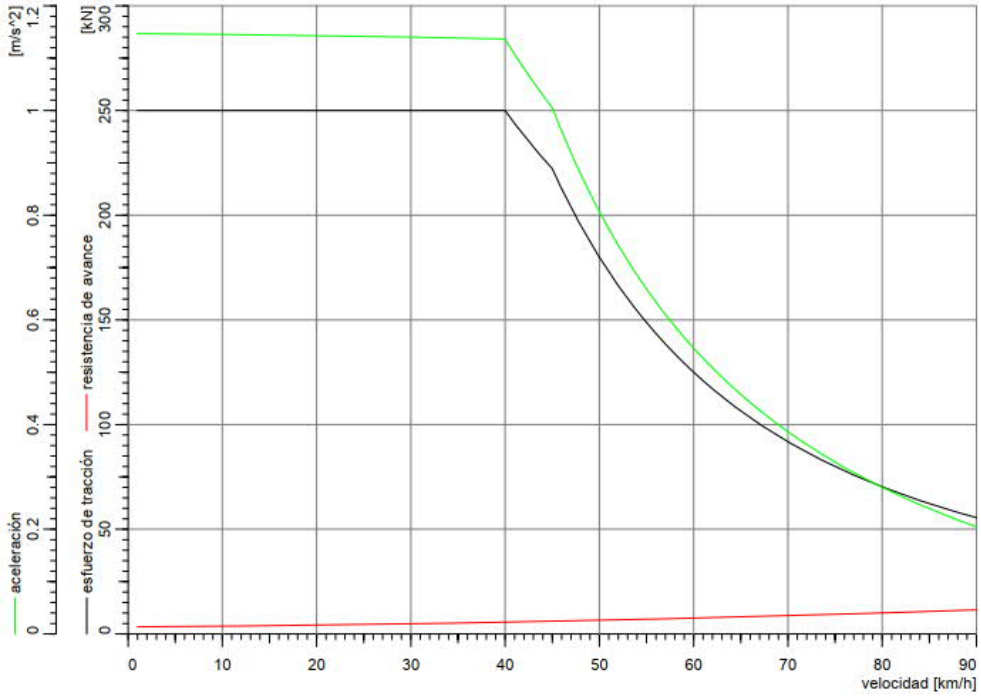

Figure 4-7. Tractive effort / Speed diagram UT113 FGC

The following equations shown are the ones used by the model present in OpenTrack software (Nash & Huerlimann, 2004) to simulate rolling stock behavior. The adhesion or friction behavior between wheel and rail is modelled by using the Curtius and Kniffler formula:

$$\mu_{\mathrm{H}} = \frac{7.5}{V+44} + 0{,}161 \qquad (4\text{-}1)$$

Where:

μ_H: Friction coefficient

V: Speed in km/h

The resistance to the advance of the train results from the addition of the traction and acceleration resistances:

$$R = R_F + R_a \quad (4\text{-}2)$$

Where:

R_F: Traction resistance [N]

R_a: Acceleration resistance [N]

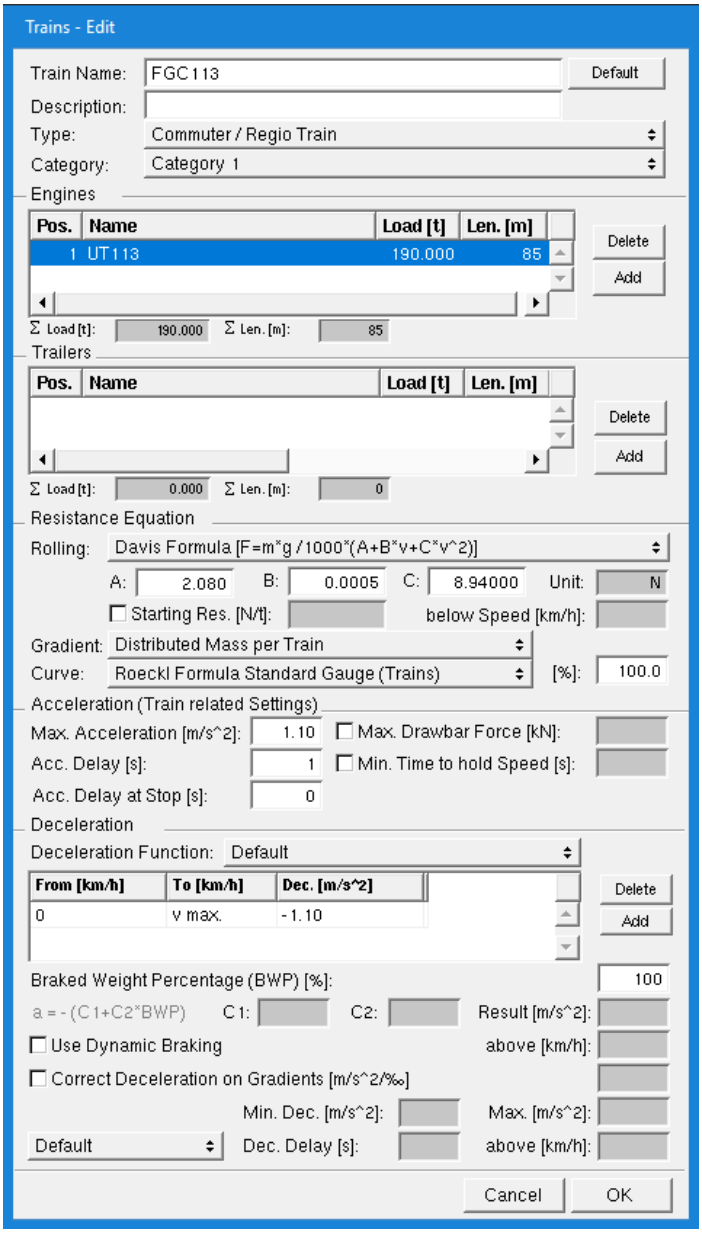

Figure 4-8. Train simulated parameters UT113 FGC

Acceleration resistance is calculated using:

$$R_{\mathrm{A}} = \mathrm{m} \cdot \mathrm{a} \cdot (1 + 0{,}01 \cdot \rho) \quad (4\text{-}3)$$

Where:

m: Train mass [kg]

a: Acceleration [m/s^2]

ρ: Empirical mass factor

Traction resistance is composed of rolling and distance resistances:

$$R_{\mathrm{F}} = R_{\mathrm{L}} + R_{\mathrm{D}} \quad (4\text{-}4)$$

Where:

R_{L}: Rolling resistance [N]

R_{D}: Distance resistance [N]

Rolling resistance is composed of air resistance and tunnel resistance:

$$R_{\mathrm{L}} = R_{\mathrm{LZ}} + R_{\mathrm{T}} \quad (4\text{-}5)$$

When trains travel through tunnels have to bear a higher resistance due to the tunnel diameter and the surface of its walls. This is modelled using the following equation:

$$R_{\mathrm{T}} = f_{\mathrm{T}} \cdot v^2 \quad (4\text{-}6)$$

Where:

R_{T}: Tunnel resistance [N]

f_{T}: Tunnel factor [kg/m]

v: Speed [m/s]

To model the effect of the unit UT113 air resistance, the mass-dependent quadratic Davis formula has been selected:

$$r' = A + B \cdot v + C \cdot v^2 \quad (4\text{-}7)$$

$$R_{\mathrm{LZ}} = \frac{m \cdot g \cdot r'}{1000} \quad (4\text{-}8)$$

Where:

R_{LZ}: Air resistance [N]

r': Special air resistance [N]

m: Weight of wagons [kg]

V: Speed [m/s]

Distance resistance consists of gradient resistance and curve resistance:

$$R_{\mathrm{D}} = R_{\mathrm{G}} + R_{\mathrm{C}} \qquad (4\text{-}9)$$

Gradient resistance is the part of the train mass working in the opposite direction to the movement of the train due to the existing gradient:

$$R_{\mathrm{G}} = m \cdot g \cdot \tan(\alpha) = m \cdot g \cdot \frac{I}{1000} \qquad (4\text{-}10)$$

Curve resistance is due to the friction between the wheel flanges and the rail during the movement of the train through a curve:

$$R_{\mathrm{C}} = \frac{6{,}3}{r-55} \cdot m \qquad \text{for r}\geq 300\text{m} \qquad (4\text{-}11)$$

$$R_{\mathrm{C}} = \frac{4{,}91}{r-30} \cdot m \qquad \text{for r}< 300\text{m} \qquad (4\text{-}12)$$

Where:

R_{G}: Gradient resistance [N]

R_{C}: Curve resistance [N]

r: Curve radius [m]

I: Positive gradient [‰]

m: Train mass [kg]

4.4. TRAIN MOVEMENT MODEL

The train movement is modelled by starting with the Newton's basic equation of Dynamics:

$$a = \frac{F}{m} \quad (4\text{-}13)$$

Where:

a: Acceleration [m/s^2]

m: Train mass [kg]

F: Train traction effort [N]

The train starts its movement if the Traction Effort it is applying to the rails is higher than the Traction Resistance:

$$F_{\mathrm{Z}} = Z(v) - R_{\mathrm{F}}(v, s) \quad (4\text{-}14)$$

Where:

F_{Z}: Tractive Surplus [N]

Z: Tractive Effort [N]

R_{F}: Traction Resistance [N]

v: Speed [m/s]

s: Distance [m]

From the diagram of the tractive effort/speed presented in Figure 4-7 the value of Tractive Effort Z(v) is obtained. If all Tractive Surplus is used to accelerate the train:

$$a = \frac{F_{\mathrm{Z}}}{m \cdot (1+0{,}01 \cdot \rho)} \quad (4\text{-}15)$$

F_{Z}: Tractive Surplus [N]

m: Train mass [kg]

a: Acceleration [m/s^2]

ρ: Rotary masses - Empirical mass factor

4.5. OPERATIONS MODEL

Data obtained from the real installation has been used to create the movement of trains from every origin to its destination. There are three types of levels used to define train movements and operations; the higher levels include units of the lower levels. The levels, from less to more complex, are called routes, paths and itineraries.

The lowest level of design are the routes; these are descriptions of train movements formed by several vertex placed in the same direction of train movement. This movement allows movement of the train from one element to another. These elements are typically main signals and during their occupation by a train they are not available to any other movement. Routes link together signals, points and segments of track to form possible basic movements a train can perform in the installation.

An example of this definition can be found in Figure 4-9, which shows all possible routes from the signal 218 in Gràcia station. The route definition includes the average gradient present, length of the movement from origin to destination and the time required by the interlocking to lock and release it. This processing time is highly dependent on the type of technology used by the interlocking; in general, electronic interlockings tend to be faster than electrical older relay-based ones. Electronic interlockings speed depend on the speed of their main processor and also generally the newer they are the faster they process the rungs forming their signaling code. But this speed is also dependent on the size of the installation managed by the interlocking and therefore the number of elements under the control of it. So, the times required to lock and release a route are variable for every type of installation and approximative values need to be defined in every case to simulate the behavior of the real installation.

Also, the signal aspects and release procedure for the route is defined as shown in Figure 4-9 as well as the approach zone of the signal ending the route. This means that the train will reduce its speed within the approach zone to match the maximum speed value allowed at the beginning of the approach zone set.

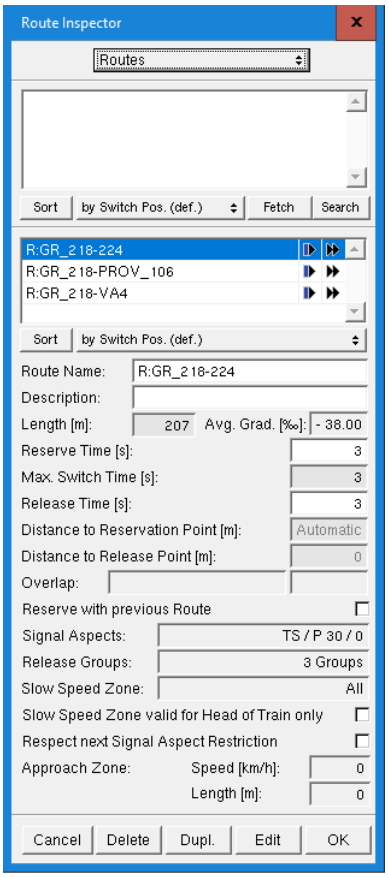

Figure 4-9. Example of routes definition: Routes from signal 218 in Gràcia

The following level of signaling design uses paths, which are sets of one or various sequential routes used together and grouped to form longer movements in the same direction. These movements are for example the ones required to move a train from a certain station to the following one, so they may include various elements like signals, track circuits and points. An example of a path definition is shown in Figure 4-10.

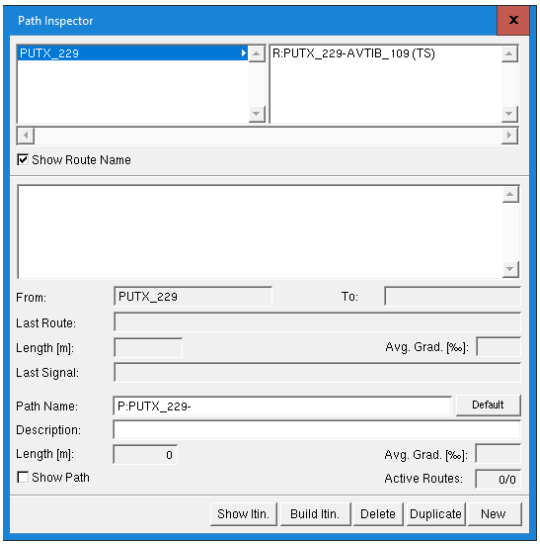

Figure 4-10. Example of path definition: Path from signal 229 in Putxet

The last level of signaling design uses itineraries, which are sets of one or various sequential paths grouped to form for example longer movements or even the operation of a complete line. Itineraries therefore can group paths that are designed in different directions. An example of an itinerary list is shown in Figure 4-11.

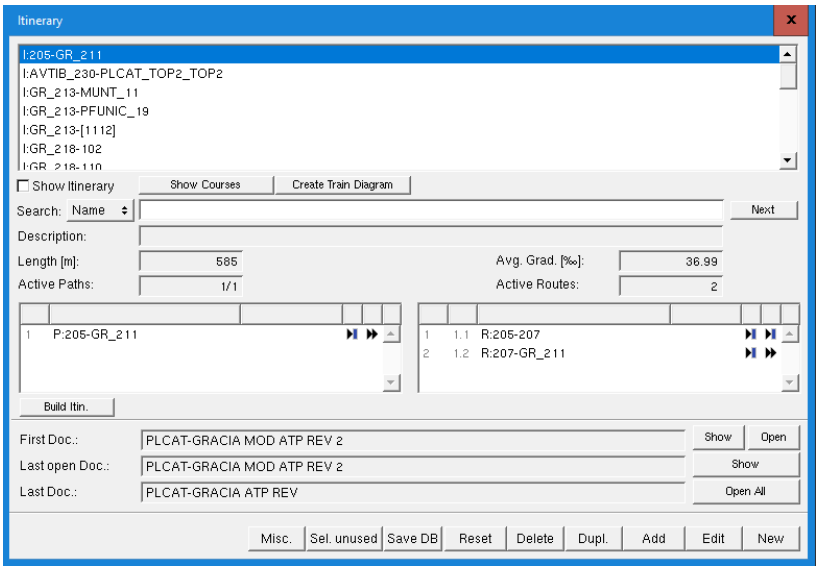

Figure 4-11. List of defined Itineraries

Itineraries are then associated to train operations through the creation of Courses, which are Itineraries associated to a specific kind of Rolling Stock and timetable definition. The Courses definition is shown in Figure 4-12 and it shows that also its speed type and performance parameters could be defined.

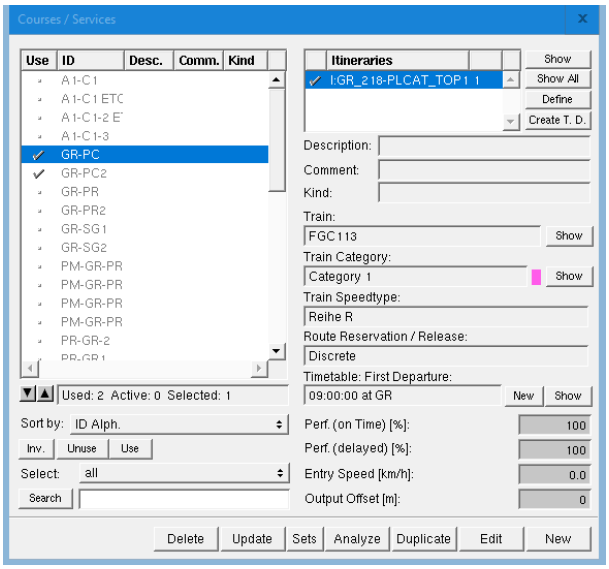

Figure 4-12. List of courses available

The timetable definition includes the list of stations included in the Itinerary and defines its arrival and departure times, dwell times at stations, stops and other

adjustments like connections to other itineraries, split and joining of trains. An example of this management window is shown in Figure 4-13.

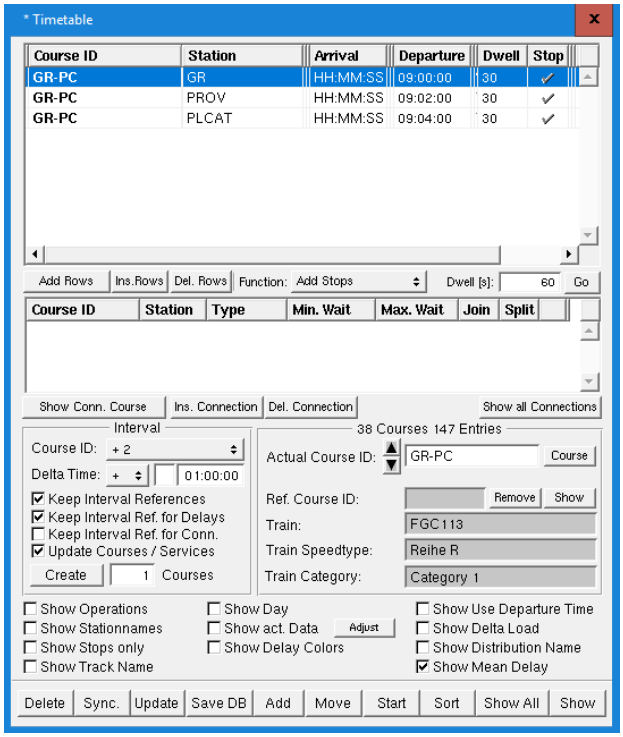

Figure 4-13. Example of timetable management window: Itinerary from Gràcia to Plaça Catalunya

CHAPTER 5

CONCLUSIONS, CONTRIBUTIONS, PUBLICATIONS AND FUTURE WORKS

5.1 CONCLUSIONS AND CONTRIBUTIONS

This section collects the main conclusions obtained and contributions generated that have led to the development of this thesis. Also, future works are proposed as a continuation of it.

FUZZY MAXIMUM CAPACITY AND OCCUPANCY TIME RATE MEASUREMENTS IN URBAN RAILWAY LINES

The main goal of this work is to improve urban railway lines capacity analysis considering the uncertainty associated to dwell times. In these types of lines, dwell times have an important impact on capacity because there are frequent stops, and running times are quite stable due to the use of automatic driving systems.

New capacity measures have been proposed: The Fuzzy Maximum Capacity and the Fuzzy Occupancy Time Rate. They are based on the maximum capacity and occupancy time rates defined in UIC (2013) (timetable compression method), including the uncertainty associated with dwell times modeled as fuzzy numbers.

Three practical problems from the perspective of the traffic operator have been presented and solved applying the proposed model, by means of the alpha-cut arithmetic: (1) Is the operative capacity achievable?, (2) Does the operative capacity keep enough reliability margins?, (3) Which is the highest operative capacity that fulfills the recommended UIC Occupancy Time margins? Problems (1) and (2) are solved by calculating the degree of compliance in terms of possibility and necessity measures, while the third one calculates the maximum operative capacity that achieves the UIC robustness requirement with a given level of possibility or necessity as a target.

The proposed model has been applied to the section Gràcia-Sarrià of the Spanish railway operator FGC. The model uses a railway simulator that enables the timetable compression method to obtain minimum conflict-free cycle times of the section under study.

It has been shown that the proposed method provides more information to the railway operator than the standard UIC method that does not include uncertainty regarding dwell times. The model permits as well adjusting the level of fulfillment of the UIC time margins to calculate the operative capacity. Furthermore, the sensitivity of the transport capacity to the uncertainty level for these input parameters of the model has been analyzed.

DESIGN OF INDICATORS TO GUIDE CAPACITY IMPROVEMENTS IN URBAN RAILWAY LINES

In general, Railway capacity increase is one of the great challenges faced by planners and infrastructure managers. To allow them to choose the most cost-effective solution among different alternatives it becomes vital to have suitable tools available.

In this work, two different indicators have been presented. These indicators ease the decision process among different installation alternatives. The indicator I_{DAP} is a measure of capacity under disturbed conditions; it is the expected value for the departure-arrival interval of trains in a node. On the other hand, the indicator T_{RD} represents the loss of commercial speed caused by the speed reduction generated in the signaling system to protect routes of other trains in the installation or other constraints.

A case study with the application of the described model and its indicators has been presented in this work, based on Barcelona-Vallès line of FGC.

The railway line Barcelona-Vallès of the Spanish operator FGC is of great importance to the metropolitan region of Barcelona. The increase in passenger demand puts more pressure on the capacity of the line thus all possibilities need to be explored in order to squeeze more capacity from the current signaling system before getting involved in costly infrastructure upgrades

The results of the application of the model show a reliable technique that can be used to improve the signaling of railway systems in order to increase its capacity levels. In table 3-8 the compared values between the original case and the proposed resignaling solution discussed in section 3.4 are presented. The redesigned proposal clearly improves the values of Minimum departure-arrival itinerary times I_{DAmin} and Average Disturbed Interval I_{Dap} .

Also, Disturbed Train Running Times T_{RD} and Disturbed Capacity C_D value are clearly improved. All these changes enable more capacity in the section without the implementation of expensive changes, just with the displacement of three track circuits frontiers.

The aforementioned indicators presented can be used to improve decisions taken in the

field of design and redesign of signaling systems and therefore support the cost-benefit analysis process previous to a sound infrastructure investment. There are many application possibilities available, from choosing between different signaling design alternatives by applying the indicators from scratch in Greenfield projects to selecting the most cost-effective solution to increase capacity in Brownfield Projects.

5.2 PUBLICATIONS

The studies carried out in the frame of this thesis work have yielded the following publications:

JCR Journals

Navarro, L. M., Fernandez-Cardador, A., & Cucala, A. P. (2018). Fuzzy maximum capacity and occupancy time rate measurements in urban railway lines. European Transport Research Review, 10(2), 1–14. https://doi.org/10.1186/s12544-018-0335-3

JCR Journals Awaiting publication (under review)

Navarro, L. M., Fernandez-Cardador, A., & Cucala, A. P. (2020). Design of indicators to guide capacity improvements in urban railway lines. European Transport Research Review

5.3 FUTURE WORK

In this section, some research lines are proposed to continue the work presented in this thesis.

FUZZY MAXIMUM CAPACITY AND OCCUPANCY TIME RATE MEASUREMENTS IN URBAN RAILWAY LINES

Regarding the Fuzzy Maximum Capacity and Occupancy Time Rate measurements, the work could be expanded with the following additional works:

- Other infrastructure topologies like suburban railway lines or lines equipped with CBTC systems. This would allow enriching the knowledge of the procedures and also establishing new reference values for every type of different line topologies and technologies.

- Extending the application of Fuzzy techniques to other variables beyond Dwell Times. For example, by applying Fuzzy numbers to weight present in the train coaches as this could be used to introduce uncertainty in the time required by train movements.

- Analyze the feasibility of creating a custom membership function to define the Fuzzy Dwell Times.

DESIGN OF INDICATORS TO GUIDE CAPACITY IMPROVEMENTS IN URBAN RAILWAY LINES

Regarding the Design of Indicators to guide Capacity Improvements in Urban Railway Lines, the scope of the study could be extended with the following proposed additional works:

- Extending the works to other types of infrastructures like suburban and high-speed railway lines. Also, the use of Dynamic Indicators could be extended to nodes like junctions or terminus stations.

- Adding other installations with different signaling technologies that could also be tested like ERTMS level 2 or CBTC.

- Developing an assisted design model of urban railway signaling systems based on the indicators presented in this work. It could include automatic optimization processes, like accurate track circuit sizing.

- Incorporate as a design variable in the improvement of capacity in disturbed lines the regulation of speed provided by the ATO system.

CHAPTER 6: REFERENCES

Abril, M., Barber, F., Ingolotti, L., Salido, M. A., Tormos, P., & Lova, A. (2008). An assessment of railway capacity. Transportation Research Part E: Logistics and Transportation Review, 44(5), 774–806.

Balaji, P. G., & Srinivasan, D. (2011). Type-2 fuzzy logic based urban traffic management. Engineering Applications of Artificial Intelligence, 24(1), 12-22.

Ballis, a, Liberis, K., & Moschovou, T. (2004). Investigating the capacity of a Metro line by means of a simulation model. Proceedings of the Institution of Mechanical Engineers, Part F: Journal of Rail and Rapid Transit, 218(1), 67–78.

Becker, M., & Schreckenberg, M. (2018). Case Study: Influence of Stochastic Dwell Times on Railway Traffic Simulations. IEEE Conference on Intelligent Transportation Systems, Proceedings, ITSC, 2018-Novem(5550), 1227–1233. https://doi.org/10.1109/ITSC.2018.8569934

Bellman, R. E., & Zadeh, L. A. (1970). Decision Making in a Fuzzy Environment. (Lotfi A Zadeh, K.-S. Fu, K. Tanaka, & M. Shimura, Eds.)Management Science, 17(4), 141-164. Academic Press. Retrieved from http://linkinghub.elsevier.com/retrieve/pii/S0898122199000590

Buchmueller, S., Weidmann, U., & Nash, A. (2008). Development of a dwell time calculation model for timetable planning, 103, 525–534. http://doi.org/10.2495/CR080511

Burdett, R. L. (2015). Multi-objective models and techniques for analysing the absolute capacity of railway networks. European Journal of Operational Research, 245(2), 489–505.
Chanas, S., Kołodziejczyk, W., & Machaj, A. (1984). A fuzzy approach to the transportation problem. Fuzzy Sets and Systems.

Burdett, R. L. (2016). Optimisation models for expanding a railway's theoretical capacity. European Journal of Operational Research, 251(3), 783–797. https://doi.org/10.1016/j.ejor.2015.12.033

Caprara, A., Fischetti, M., & Toth, P. (2002). Modeling and Solving the Train Timetabling Problem. Operations Research, 50(5), 851–861.

Carey, M. (1994). A model and strategy for train pathing with choice of lines, platforms, and routes. Transportation Research Part B, 28(5), 333–353.

Chanas, S., & Kasperski, A. (2001). Minimizing maximum lateness in a single machine scheduling problem with fuzzy processing times and fuzzy due dates. Engineering Applications of Artificial Intelligence, 14(3), 377-386.

Chang, C.S., Thia, B.S., 1996. Online rescheduling of mass rapid transit systems: fuzzy expert system approach. IEE Proc. Electr. Power Appl. 143 (4), 307–316.

Chu, W.-J., Zhang, X.-C., Chen, J.-H., & Xu, B. (2015). An ELM-Based Approach for Estimating Train Dwell Time in Urban Rail Traffic. Mathematical Problems in Engineering, 2015(473432).

Cucala, A. P., Fernández, A., Sicre, C., & Domínguez, M. (2012). Fuzzy optimal schedule of high speed train operation to minimize energy consumption with uncertain delays and drivers behavioral response. Engineering Applications of Artificial Intelligence, 25(8), 1548–1557.

Dicembre, a., & Ricci, S. (2011). Railway traffic on high density urban corridors: Capacity, signalling and timetable. Journal of Rail Transport Planning and Management, 1(2), 59–68.

Domínguez, M., Fernández, A., Cucala, A. P., & Lukaszewicz, P. (2011). Optimal design of metro automatic train operation speed profiles for reducing energy consumption. Proceedings of the Institution of Mechanical Engineers, Part F: Journal of Rail and Rapid Transit, 225(5), 463–473.

Dubois, D., & Prade, H. (1983). Ranking fuzzy numbers in the setting of possibility theory. Information Sciences, 30(3), 183–224.

Fay, A. (2000). A fuzzy knowledge-based system for railway traffic control. Engineering Applications of Artificial Intelligence, 13(6), 719–729.

Gašparík, J., Abramović, B., & Zitrický, V. (2018). Research on dependences of railway infrastructure capacity. Tehnicki Vjesnik, 25(4), 1190–1195. https://doi.org/10.17559/TV-20160917192247

Goverde, R. M. P., Corman, F., & D'Ariano, A. (2013). Railway line capacity consumption of different railway signalling systems under scheduled and disturbed conditions. Journal of Rail Transport Planning and Management, 3(3), 78–94.

Hansen, I. A. (2009). Railway network timetabling and dynamic traffic management. In 2nd International Conference on Recent Advances in Railway Engineering (ICRARE-2009) Iran university of science and Technology Tehran I.R. Iran -Sep 27-28, 2009, Tehran, Iran, pp. 135–145.

Haramina, H., & Talan, I. (2018). Improvement of suburban railway services by infrastructure and timetable modifications based on simulation modelling. Transport problems, 13(3), 15–27. https://doi.org/10.20858/tp.2018.13.3.2

Higgins, A., Kozan, E., & Ferreira, L. (1996). Optimal scheduling of trains on a single line track. Transportation Research Part B: Methodological, 30(2), 147–158.

Huang, P., Wen, C., Peng, Q., Jiang, C., Yang, Y., & Fu, Z. (2019). Modeling the Influence of Disturbances in High-Speed Railway Systems. Journal of Advanced Transportation, 2019(2), 1–13. https://doi.org/10.1155/2019/8639589

Isaai, M. T., Kanani, A., Tootoonchi, M., & Afzali, H. R. (2011). Intelligent timetable evaluation using fuzzy AHP. Expert Systems with Applications, 38(4), 3718–3723.
Jiang, Z., Xie, C., Ji, T., & Zou, X. (2015). Dwell time modelling and optimized simulations for crowded rail transit lines based on train capacity. Promet - Traffic&Transportation, 27(2), 125–135.

Jensen, L. W., Landex, A., Nielsen, O. A., Kroon, L. G., & Schmidt, M. (2017). Strategic assessment of capacity consumption in railway networks: Framework and model. Transportation Research Part C: Emerging Technologies, 74, 126–149. https://doi.org/10.1016/j.trc.2016.10.013

Jovanovic, D., & Harker, P. T. (1991). Tactical Scheduling of Rail Operations: The SCAN I System. Transportation Science, 25(1), 46–64. http://doi.org/10.1287/trsc.25.1.46,

Kecman, P., & Goverde, R. M. P. (2015). Predictive modelling of running and dwell times in railway traffic. Public Transport, 7(3), 295–319. http://doi.org/10.1007/s12469-015-0106-7

Kittelson & Associates, Parsons Brinckerhoff, KFH Group, Texas A&M Transportation Institute, & Arup. (2013). Transit Capacity and Quality of Service Manual. TCRB Report 165, 52.

Kontaxi, E., & Ricci, S. (2010). Railway capacity analysis: Methodological framework and harmonization perspectives. In Proceedings of the 12th World Conference on Transportation Research, Lisbon, pp. 1–21.
Krueger, H. (1999). Parametric Modeling in Rail Capacity Planning. In WSC'99. 1999 Winter Simulation Conference Proceedings., Vol. 2, pp. 1194–1200.

De Kort, A. F., Heidergott, B., & Ayhan, H. (2003). A probabilistic (max, +) approach for determining railway infrastructure capacity. European Journal of Operational Research, 148(3), 644–661.

Jiang, Z., Xie, C., Ji, T., & Zou, X. (2015). Dwell time modelling and optimized simulations for crowded rail transit lines based on train capacity. Promet - Traffic - Traffico, 27(2), 125–135. http://doi.org/10.7307/ptt.v27i2.1487

Landex, Alex; Kaas, Anders H.; Schittenhelm, Bernd Hermann; Schneider-Tilli, J. (2006). Evaluation of railway capacity. In Proceedings of Trafficdays, pp. 1–22.

Landex, A. (2012). Network effects in railways. WIT Transactions on the Built Environment, 127, 391–402.

Lai, Y. C., & Wang, S. H. (2012). Development of analytical capacity models for conventional railways with advanced signaling systems. Journal of Transportation Engineering, 138(7), 961–974. https://doi.org/10.1061/(ASCE)TE.1943-5436.0000388

Li, D., Daamen, W., & Goverde, R. M. P. (2016). Estimation of train dwell time at short stops based on track occupation event data: A study at a Dutch railway station. Journal of Advanced Transportation. http://doi.org/10.1002/atr.1380

Ljubaj, I., Mlinarić, T. J., & Radonjić, D. (2017). Proposed Solutions for Increasing the Capacity of the Mediterranean Corridor on Section Zagreb - Rijeka. Procedia Engineering, 192, 545–550. https://doi.org/10.1016/j.proeng.2017.06.094

Ljubaj, I., Mlinarić, T. J., Lezaić, T., & Starčević, M. (2018). The possibility of capacity increase on the modernised and electrified railway line R201 along the Zaprešić-Zabok section. MATEC Web of Conferences, 235, 8–11. https://doi.org/10.1051/matecconf/201823500009

Ljubaj, I., & Mlinarić, T. J. (2019). The Possibility of Utilising Maximum Capacity of the Double-Track Railway By Using Innovative Traffic Organisation. Transportation Research Procedia, 40, 346–353. https://doi.org/10.1016/j.trpro.2019.07.051

Luteberget, B., Claessen, K., & Johansen, C. (2019). Design-Time Railway Capacity Verification using SAT modulo Discrete Event Simulation. 2018 Formal Methods in Computer Aided Design (FMCAD), 1–9. https://doi.org/10.23919/fmcad.2018.8603003

Malavasi, G., Molkova, T., Ricci, S., & Rotoli, F. (2014). A synthetic approach to the evaluation of the carrying capacity of complex railway nodes. Journal of Rail Transport Planning and Management, 4(1-2), 28–42. doi:10.1016/j.jrtpm.2014.06.001

Marcianò, F. A.; Pollon, S.; Rivoli, P. (2019). Operation analyses on capacity enhancement for a regional railway line in UK through the implementation of the ERTMS/ETCS Level 2 HD signalling system. Advances in Transportation Studies an International Journal 2019 Special Issue, 3.

Medeossi, G., Longo, G., & de Fabris, S. (2011). A method for using stochastic blocking times to improve timetable planning. Journal of Rail Transport Planning and Management, 1(1), 1–13.

Milinković, S., Marković, M., Vesković, S., Ivić, M., & Pavlović, N. (2013). A fuzzy Petri net model to estimate train delays. Simulation Modelling Practice and Theory, 33, 144–157.

Mussone, L., & Wolfler Calvo, R. (2013). An analytical approach to calculate the capacity of a railway system. European Journal of Operational Research, 228(1), 11-23.

Nalmpantis, D., Roukouni, A., Genitsaris, E., Stamelou, A., & Naniopoulos, A. (2019). Evaluation of innovative ideas for Public Transport proposed by citizens using Multi-Criteria Decision Analysis (MCDA). European Transport Research Review, 11(1). https://doi.org/10.1186/s12544-019-0356-6

Nash, A., & Huerlimann, D. (2004). Railroad simulation using OpenTrack. Computers in Railways IX, 45–54.

OECD/ITF (2017), ITF Transport Outlook 2017, OECD Publishing, Paris. http://dx.doi.org/10.1787/9789282108000-en

Ortega Riejos, F. a., Barrena, E., Canca Ortiz, J. D., & Laporte, G. (2015). Analyzing the theoretical capacity of railway networks with a radial-backbone topology. Transportation Research Part A: Policy and Practice. doi:10.1016/j.tra.2015.03.018

Parkinson, T. and Fisher, I. (1996). TCRP Report 13: Rail Transit Capacity. TRB, National Research Council, Washington, DC.

Perkins, A., Ryan, B., & Siebers, P. (2014). Modelling and Simulation of Rail Passengers to Evaluate Methods To Reduce Dwell Times. In 14th International Conference on Modeling and Applied Simulation, pp. 132–141.

Reinhardt, L. B., Pisinger, D., & Lusby, R. (2018). Railway capacity and expansion analysis using time discretized paths. Flexible Services and Manufacturing Journal, 30(4), 712–739. https://doi.org/10.1007/s10696-017-9292-8

Robert, L., Burdett, R. L., & Kozan, E. (2006). Techniques for Absolute Capacity Determination in Railways, 40, 616–632.

Rosell, Francisca; Codina, E. (2020). A model that assesses proposals for infrastructure improvement and capacity expansion on a mixed railway network. Transportation Research Procedia, 47, 441–448. https://doi.org/10.1016/j.trpro.2020.03.119

Salido, M. A., Tarazona, S. (n.d.). Robustness in Railway Timetables. In 7th World Congress on Intelligent Control and Automation, 2008, Chongqing, China. Retrieved from http://arrival.cti.gr/uploads/Documents.0125/ARRIVAL-TR-0125.pdf

San, H. P., & Masirin, M. I. M. (2016). Train Dwell Time Models for Rail Passenger Service. In MATEC Web of Conferences, Vol. 47, pp. 3005-1–6.

Shekhar, S., Singh, A., Belur, M. N., & Rangaraj, N. (2019). Development of a railway junction simulator for evaluation of control strategies and capacity utilization optimization. 2019 5th Indian Control Conference, ICC 2019 - Proceedings, (Icc), 260–265. https://doi.org/10.1109/INDIANCC.2019.8715629

UIC. (1996). Leaflet 405 OR- Links between Railway Infrastructure Capacity and the Quality of Operations 1st Edition.

UIC. (2008). Influence of ETCS on line capacity - Generic study.

UIC. (2010). Influence of the European Train Control System (ETCS) on the capacity of nodes.

UIC. (2013). Code 406 Capacity 2nd Edition.

Yang, L., Li, K., & Gao, Z. (2009). Train timetable problem on a single-line railway with fuzzy passenger demand. IEEE Transactions on Fuzzy Systems, 17(3), 617–629.

Zhang, H., Pu, H., Schonfeld, P., Song, T., Li, W., Wang, J., … Hu, J. (2020). Multi-objective railway alignment optimization considering costs and environmental impacts. Applied Soft Computing Journal, 89, 106105. https://doi.org/10.1016/j.asoc.2020.106105

Zhang, Q., Han, B., & Li, D. (2008). Modeling and simulation of passenger alighting and boarding movement in Beijing metro stations. Transportation Research Part C: Emerging Technologies, 16(5), 635–649.

Zhang, H., Pu, H., Schonfeld, P., Song, T., Li, W., Wang, J., & Hu, J. (2020). Multi-objective railway alignment optimization considering costs and environmental impacts. Applied Soft Computing Journal, 89, 106105. https://doi.org/10.1016/j.asoc.2020.106105

Zhong, M. (2018). Analyzing and Evaluating Infrastructure Capacity of Railway Passenger Station by Mesoscopic Simulation Method. 2018 International Conference on Intelligent Rail Transportation (ICIRT), 1–5. https://doi.org/10.1109/ICIRT.2018.8641593

Zieger, S., Weik, N., & Nießen, N. (2018). The influence of buffer time distributions in delay propagation modelling of railway networks. Journal of Rail Transport Planning and Management, 8(3–4), 220–232. https://doi.org/10.1016/j.jrtpm.2018.09.001